

AD-A261 729



PL-TR-92-2307

DTIC
ELECTE
FEB 24 1993
S C D

(2)

**DETAILED COMPONENT DESIGN FOR A COMPACT
ENVIRONMENTAL ANOMALY SENSOR (CEASE)**

**Alan C. Huber
John O. McGarity
Paul Okun
John A. Pantazis
David Sperry**

**Hugh Anderson
Douglas Potter**

**AMPTEK, INC.
6 De Angelo Drive
Bedford, MA 01730**

16 November 1992

Scientific Report No. 2

93-03858



APPROVED FOR PUBLIC RELEASE; DISTRIBUTION UNLIMITED



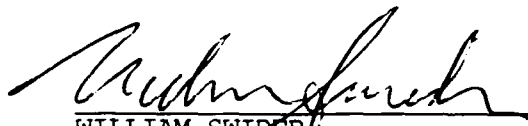
**PHILLIPS LABORATORY
Directorate of Geophysics
AIR FORCE MATERIEL COMMAND
HANSCOM AIR FORCE BASE, MA 01731-5000**

93 223 114

This technical report has been reviewed and is approved for publication.


PAUL S. SEVERANCE
Contract Manager


for E. G. MULLEN
Branch Chief


WILLIAM SWIDER
Deputy Division Director

This report has been reviewed by the ESC Public Affairs Office (PA) and is releasable to the National Technical Information Service (NTIS).

Qualified requestors may obtain additional copies from the Defense Technical Information Center. All others should apply to the National Technical Information Service.

If your address has changed, or if you wish to be removed from the mailing list, or if the addressee is no longer employed by your organization, please notify PL/TSI, Hanscom AFB, MA 01731-5000. This will assist us in maintaining a current mailing list.

Do not return copies of this report unless contractual obligations or notices on a specific document requires that it be returned.

REPORT DOCUMENTATION PAGE			Form Approved OMB No. 0704-0188	
Public reporting burden for this collection of information is estimated to average 1 hour per response, including the time for reviewing instructions, searching existing data sources, gathering and maintaining the data needed, and completing and reviewing the collection of information. Send comments regarding this burden estimate or any other aspect of this collection of information, including suggestions for reducing this burden, to Washington Headquarters Services, Directorate for Information Operations and Reports, 1215 Jefferson Davis Highway, Suite 1204, Arlington, VA 22202-4302, and to the Office of Management and Budget, Paperwork Reduction Project (0704-0188), Washington, DC 20503.				
1. AGENCY USE ONLY (Leave blank)		2. REPORT DATE 16 November 1992		3. REPORT TYPE AND DATES COVERED Scientific Report No. 2
4. TITLE AND SUBTITLE Detailed Component Design for a Compact Environmental Anomaly Sensor (CEASE)			5. FUNDING NUMBERS PE 63410F PR 2823 TA 01 WU AC Contract F19628-90-C-0159	
6. AUTHOR(S) Alan C. Huber John A. Pantazis *Douglas Potter John O. McGarity David Sperry Paul Okun *Hugh Anderson				
7. PERFORMING ORGANIZATION NAME(S) AND ADDRESS(ES) AMPTEK, INC. 6 De Angelo Drive Bedford, MA 01730			8. PERFORMING ORGANIZATION REPORT NUMBER	
9. SPONSORING/MONITORING AGENCY NAME(S) AND ADDRESS(ES) PHILLIPS LABORATORY Hanscom AFB, MA 01731-5000 Contract Manager: Capt. Paul Severance / GPSP			10. SPONSORING/MONITORING AGENCY REPORT NUMBER PL-TR-92-2307	
11. SUPPLEMENTARY NOTES * SAIC NW, 13400B Northrup Way, Suite 36, Bellevue, WA 98005				
12a. DISTRIBUTION/AVAILABILITY STATEMENT Approved for public release. Distribution unlimited.			12b. DISTRIBUTION CODE	
13. ABSTRACT (Maximum 200 words) As the size and sophistication of spacecraft have increased, anomalies in operational performance caused by the interaction of the energetic-particle population and the spacecraft have likewise increased. The Compact Environmental Anomaly Sensor (CEASE) is being developed as a small, low-power device to monitor space "weather" and provide autonomous warning of conditions that could cause operational anomalies. Based on Amptek's sensor-design and trade-off studies for CEASE, a dosimeter set consisting of solid-state detectors behind aluminum absorbers (of several thicknesses) has been chosen. The outputs of the detectors are fed into algorithms that warn of certain anomalies: (1) surface dielectric charging, (2) deep dielectric charging, (3) total radiation dose behind 0.035 g/cm ² , (4) total dose behind 0.41 g/cm ² , and (5) single event upsets. From seven quantities derived by algorithm processing, eight warning levels (1, 3, 100...3000 x base) are obtained for each of the five anomalies. Level flags can then be selected for a particular application. For such a CEASE instrument, we estimate a volume of 64 in ³ (4-inch cube), a weight of 2 pounds, and power dissipation of 2 watts.				
14. SUBJECT TERMS Compact Environmental Anomaly Sensor, CEASE, Surface Charging, Deep Dielectric Charging, Single Event Upsets, Radiation Dose Effects.			15. NUMBER OF PAGES 56	
			16. PRICE CODE	
17. SECURITY CLASSIFICATION OF REPORT Unclassified	18. SECURITY CLASSIFICATION OF THIS PAGE Unclassified	19. SECURITY CLASSIFICATION OF ABSTRACT Unclassified	20. LIMITATION OF ABSTRACT SAR	

CONTENTS

1. Introduction.....	1
2. Purpose of CEASE.....	3
2.1. Anomalies and Causes	3
2.2. Environments to be Sensed	6
3. Cease Detectors	7
3.1. For Charging Environments	7
3.1.1. Trade Studies on Various Sensors	7
3.1.2. Solid State Telescope Adopted.....	8
3.1.2.1. Response	8
3.1.2.1.1. Energy.....	8
3.1.2.1.2. Counting Rate and Geometric Factor ...	10
3.1.2.2. Backgrounds.....	11
3.2. Detector for Radiation Dose	12
3.2.1. Trade Studies on Various Sensors	12
3.2.2. Adopted Sensor.....	12
3.2.2.1. Response	14
3.2.2.1.1. Energy.....	14
3.2.2.1.2. Counting Rate and Geometric Factor ...	15
3.2.2.2. Backgrounds	15
3.3. Temperature Controlled MOSFET Dosimeter	15
4. Warning Flags	17

DTIC QUALITY INSPECTED 3

Accession For	
NTIS	CRA&I
DTIC	TAB
Unannounced Justification	
By	
Distribution /	
Availability Codes	
Dist	Avail and / or Special
A-1	

4.1. Sensor Input to Warning Logic	17
4.2. Warning Algorithms.....	18
4.3. Comments.....	19
5. IV Hardware Implementation	20
5.1. Signal Processing Electronics.....	20
5.1.1. Charge Sensitive Preamplifier.....	21
5.1.2. Shaping amplifiers and gain stages	21
5.1.3. Stacked discriminators.....	21
5.1.4. Dose Integrator Circuit.....	21
5.2. Power Supplies	22
5.3. Overview of CEASE Control Electronics.....	29
5.3.1. CPU Configuration.....	30
5.3.1.1. Hybrid Processor	30
5.3.1.2. Microprocessor.....	31
5.3.1.3. Memory.....	31
5.3.1.4. RS-422 Interface.....	31
5.3.1.5. Miscellaneous.....	32
5.3.2. Gate Array	32
5.3.3. Telemetry	34
6. Software.....	34
7. CEASE Specifications (weight, power, and envelope).....	34
8. Proposed Development Schedule.....	35
Appendix I. Response Curves for Various Telescope Parameters	39

1. Introduction

Thirty-four years of space flight experience has demonstrated that the space environment contains more hazards than just vacuum and extreme temperatures. The earliest United States spacecraft, Explorer I, encountered the radiation belts that surround the Earth. Later spacecraft experienced other effects of the population of charged particles that flow around the field lines of the Earth's magnetic poles. As our experience grew and the number, size, and sophistication of our satellites and spacecraft increased, we accumulated a history of anomalous spacecraft behavior. We now know that many of these anomalies are triggered by interactions between the spacecraft and the energetic particle populations that form the plasma environment of outer space.

The plasma conditions that threaten spacecraft operations are not confined to the near Earth region, but have been observed throughout the solar system by our various planetary probes. Some of these conditions can be addressed by appropriate design techniques such as radiation hardened electronics, shielding of sensitive devices, avoiding structural features that may allow exposed high electric fields, and materials selection that minimize outgassing, ablation, or condensable products. Spacecraft design with these environmental features as well as the thermal extremes and vacuum effects in mind is now the accepted practice.

The space environment is not homogeneous in either time or region. Interplanetary space, the planetary magneto sheath, inner magnetosphere, plasma sheet, and magneto tail, all are plasma structures that evolve from interactions of the solar wind with planetary magnetic fields. The plasma populations of these regimes can vary by many orders of magnitude. Likewise, solar activity in the form of flares and sunspots can trigger variations of many orders of magnitude in these regions.

Modern spacecraft design minimizes susceptibility to this dynamic and somewhat unpredictable environment, but it does not eliminate all anomalies. Space "weather" is just as volatile as terrestrial weather. On Earth we have learned to design for the weather, even its extremes, but we still find it necessary to attempt some type of weather forecasting to help us schedule our activities in periods that are stable and safe. A similar "weather" forecasting capability is desirable for spacecraft. If a spacecraft has an accurate forecast, it can inhibit or modify its activities to minimize the probability of environmental interference.

For example, an orbital adjustment using thrusters may be delayed if there is a higher than usual probability of a Single Event Upset (SEU) which could cause catastrophic confusion if one occurred during critical maneuvering. Similarly, if the cumulative radiation dosage of the spacecraft reached levels that may reduce the reliability of some of the electronic circuitry, then some measurements may need acceleration to insure their reliability.

The CEASE Instrument is intended to be such a "weather" forecast device. It is meant to be as unobtrusive as possible, consuming as little spacecraft resources of power and mass as possible, while providing monitoring of the environment and early warning of the probability of various anomaly inducing conditions. It should be noted that CEASE is an environment monitoring device and not a scientific data collecting instrument.

2. Purpose of CEASE

2.1. Anomalies and Causes

CEASE is designed to detect conditions that may cause anomalies, that is, occurrences that may adversely affect spacecraft operation. It will do so before these conditions become so severe that anomalies actually occur, and will provide warnings or flags on which spacecraft may act to protect themselves. We provide a short summary of the nature and cause of anomalies.

Body charging occurs when the spacecraft chassis accumulates electrical charge and the whole space frame must rise to a significant potential (with respect to the surrounding plasma) in order to null the net current to it. This charging occurs even when the whole spacecraft surface is conducting and electrically connected. Body charging is caused by spacecraft emitting charge, such as in a particle beam, or when they are bombarded by kilovolt electrons such as the auroral electron flux or the hot plasma in GEO. The charging can become significant in the absence of neutralizing currents such as cooler plasma or photoelectrons ejected by sunlight.

- ◆ The consequence of body charging is that the energy spectra of arriving plasma is distorted, rendering scientific measurements complicated to interpret. A completely conducting spacecraft does not suffer from other anomalies as a result of body charging.

Differential charging occurs under the same conditions as body charging if the spacecraft exterior has sections of electrically isolated conductor. As different portions of the surface experience different currents, these separate sections may reach different equilibrium potentials.

- ◆ The consequence of differential charging is that electric fields between adjacent conducting sections may be high enough to arc and cause electrical noise. This noise, if conducted throughout the spacecraft, may act as a false signal or even damage sensitive elements.

Surface dielectric charging occurs when somewhat penetrating particles bombard exposed dielectrics and stop in them. If the rate of charge buildup exceeds leakage through the dielectric, the resulting charge density may produce a very strong electric field that eventually breaks down the dielectric. Leakage depends upon the dielectric material; hence, charging may be cumulative over minutes up to many hours. Leakage increases as conductivity is enhanced by the

effect of the bombarding particles. Consequently, protons are not very effective in causing dielectric charging because they readily increase dielectric conductivity. In addition, sunlight may help discharge very shallow deposits of charge. The result of these factors is that surface charging occurs when the electron flux exceeds a threshold value and sums to a fluence that exceeds a threshold. While the values vary somewhat with dielectric material, Table 1 lists typical thresholds.

- ◆ The consequences of surface dielectric charging are breakdowns within the dielectric that propagate electrical noise throughout the spacecraft.

Deep dielectric charging is produced in the same way as surface dielectric charging except that the causative electrons have enough energy to penetrate some distance into the dielectric. In some cases they may reach dielectrics that are behind conductors. An example of a buried dielectric is the insulator within a coaxial cable. Obviously the energy boundary that divides surface and deep charging particles is somewhat arbitrary. Sunlight does not mitigate deep dielectric charging.

- ◆ The consequence of deep charging are the same as of surface charging.

Total radiation dose is measured by the energy deposited in materials by charged particles passing through them. Dosage results from the totality of ionizing radiation that reaches the site of interest, and is thus strongly affected by surrounding shielding. Sufficiently high levels can damage most materials, including dielectrics and optical materials. In most cases semiconductors are the most sensitive elements on a spacecraft. Some devices experience degradation at tens of kilorads, while radiation hard devices can tolerate 10 to 100 times more. Dosage is mostly cumulative, as semiconductors self heal only a little.

- ◆ Consequences of dosage are increased leakage currents, shifted operating voltages and general degradation of performance with eventual circuit failure.

Single event upsets (SEU) result when an ionizing particle leaves enough charge (equivalently energy) in the sensitive volume of a semiconductor device to flip the logical state of the device. Generally, there is no permanent damage. The sensitive volumes are of micron size, and the required energy is 1 - 100 MeV depending upon the device. Neither electrons or protons have high enough LET (Linear Energy Transfer) to leave so much energy in a small

volume. Only more highly charged particles such as alphas (in some cases) and $Z > 2$ particles can do this. However, protons that have nuclear collisions (called stars from their appearance in photographic film) in the sensitive volume can break up a nucleus and the resulting fragments leave enough energy to cause SEUs. Protons are so much more numerous than heavier particles that these nuclear collisions are the principal cause of SEUs.

- ◆ SEU change the logical state of circuits, thereby causing disruption of operations. Spacecraft systems may have to be restarted to reset their logic. In some cases, SEUs as well as the electrical noise from discharges have caused control of a spacecraft to be lost. In much rarer cases, logical elements are set to states that can only be reset by power cycling. This is called latch-up and can cause permanent damage to some circuitry.

Orbital contamination results when one portion of a spacecraft emits molecular or particulate materials that deposit on other parts of the spacecraft. Cooled elements are especially likely to accumulate molecular deposits. Contamination is emitted from reaction control systems, from propulsion systems, and as general outgassing of materials. A related effect is the alteration and erosion of exposed materials by naturally occurring atomic oxygen and by UV in sunlight. Here, the effect depends upon the material.

- ◆ The result of contamination and the other effects is that optical, electrical, and thermal properties of surfaces may change. Over a long period this may be quite serious. Atomic oxygen erosion of hydrocarbons is significant in a week in LEO.

2.2. Environments to be Sensed

In our report at the end of the first year's study, we described means to sense contamination and its effects. However, Phillips Lab has suggested that CEASE will not measure contamination at this time, although a future version might, in principle, do so.

We believe that spacecraft body charging is not a great hazard. It and differential charging are caused by the same external conditions. Furthermore, except for the significance of thermal plasma and sunlight, the same electrons that cause dielectric charging cause body and differential charging. CEASE will warn of surface and deep dielectric charging but will not give a separate warning of body and differential charging. It will also warn of total dose and SEU.

Table 1 shows environments that cause the anomalies of concern.

Anomaly	Particle & Energy	Other Condition
Body and Differential Charging	Electrons, 5 keV - ~300 keV	No sunlight, no colder electrons
Surface Dielectric Charging	Electrons, 5 keV - ~300 keV	Fluence $> 5 \times 10^{11}/\text{cm}^2$ at flux $> 2 \times 10^6/\text{cm}^2\text{-sec}$
Deep Dielectric Charging	Electrons, > 300 keV	"
Total Dose	Electrons > 1 MeV; protons > 17 MeV; and other particles that penetrate shielding (0.4 g/cm^2 of Al)	10 krad is a level that may be significant
Single Event Upsets (SEU)	Protons able to penetrate shielding and have a nuclear interaction; heavily ionizing particles ($Z > 1$)	

Table 1. Environments that cause Anomalies

3. Cease Detectors

As mentioned earlier, our report at the end of the first year described contamination sensors. As the present version of CEASE will not sense contamination, we do not repeat that description here. The sensors described in this report measure the occurrence of the environments in Table 1. CEASE will make measurements for engineering purposes, we do not regard it as necessary to discriminate between electrons, protons, and heavier particles in all cases so long as CEASE gives an adequate warning.

3.1. For Charging Environments

3.1.1. Trade Studies on Various Sensors

In practice charging is caused by electron, not proton bombardment, with electrons of energy as low as 5 keV contributing. A windowless detector is required to sense electrons of this low energy. A Faraday cup with electrometer or an open electron multiplier would function well; the former measures the algebraic sum of all the currents flowing to it at any energy, while the latter counts all particles without regard to charge sign or energy. Hence, these detectors would be preceded by an electric or magnetic deflection system to exclude photons and unwanted particles. The deflection system would also discriminate energy and charge sign.

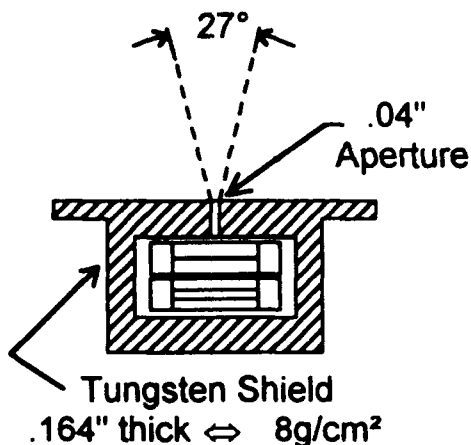
We have attempted to avoid high voltage and magnets in the interests of simplicity, thus excluding open electron multipliers and deflection systems. If low-energy electrons between 5 and 25 keV do not require direct monitoring, then CEASE may use exclusively solid state detectors that measure absorbed energy and use low, constant voltages. In order to discriminate between protons and electrons a coincidence telescope with two or more detectors must be used. We calculated the response of a two element telescope with a variety of detector and absorber thicknesses. Appendix I shows the resulting energy loss in the front and back detector, D1 and D2, as a function of incident electron and proton energy. The calculating routine uses standard range vs. energy tables.

Inspection of this family of curves shows three things:

- ◆ If particles stop in the front detector, the instrument cannot identify what type of particle it was.

- ◆ The thinner the front detector, D1, the narrower the energy range over which particles stop in that detector.
- ◆ An absorber in front of D1 shifts the minimum proton energy upward much more than it shifts minimum electron energy.

3.1.2. Solid State Telescope Adopted



As a compromise between minimum energy electrons and separation of electrons from protons, we designed a telescope with 800 $\mu\text{g}/\text{cm}^2$ absorber and detectors D1 and D2 150 μm and 1000 μm thick, respectively. Figure 1 shows this telescope. An absorber 8 g/cm² thick surrounds it to stop all but fairly high energy particles.

Figure 1. Detector Telescope

3.1.2.1. Response

3.1.2.1.1. Energy

Figure 2 shows the response of this telescope to electrons, protons, and alpha (helium) particles. From the data in this figure we plot the energy loss in D2 vs. that in D1 for each type of particle. Figure 3 shows the results. Salient features of this figure are:

- ◆ Incident particle energy varies along the curves;
- ◆ Low-energy particles that stop in D1 are shown at the bottom of the figure.

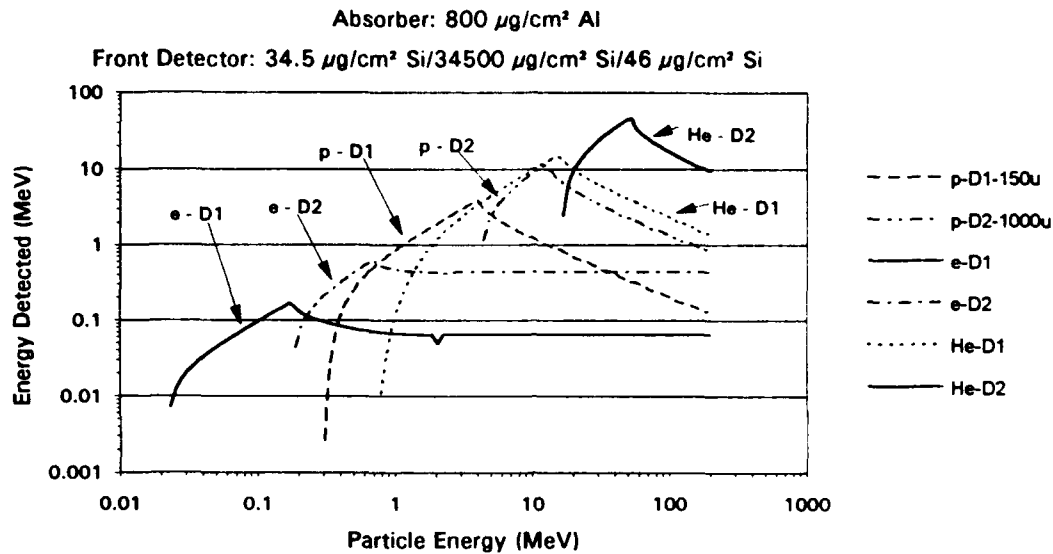


Figure 2. Telescope Response

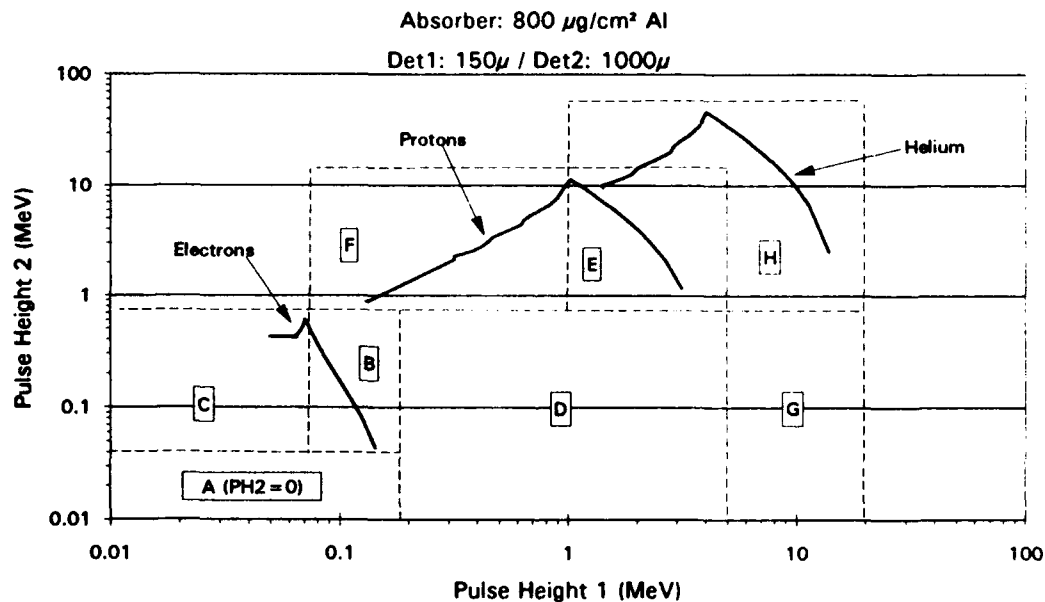


Figure 3. Detector 1 Vs. Detector 2 Responses

The D1-D2 space can be divided into bins, labeled A through H in Figure 3. Coincident energy losses falling in the various bins result from particles, as listed in Table 3. Where more than one type of particle is listed in a bin, the telescope cannot distinguish between them.

Bin	Detector 1 Pulse Height Range	Detector 2 Pulse Height Range	Particle Measured
A	25 keV - 190 keV	No coincidence - No particles penetrate	e ⁻ 25 keV - 200 keV H ⁺ 140 keV - 300 keV He 200 keV - 500 keV
B	73 keV - 190 keV	40 keV - 750 keV	e ⁻ 200 keV - 800 keV *
C	25 keV - 73 keV	40 keV - 750 keV	e ⁻ > 800 keV
D	190 keV - 5.0 MeV	25 keV - 750 keV	H ⁺ 300 keV - 4.0 MeV He 500 keV - 5.5 MeV
E	1.0 MeV - 5.0 MeV	750 keV - 13 MeV	H ⁺ 4.0 MeV - 11 MeV He 120 MeV-180+MeV*
F	73 keV - 1.0 MeV	750 keV - 13 MeV	H ⁺ > 11 MeV
G	5.0 MeV - 20 MeV	25 keV - 750 keV	He 4.0 MeV - 17 MeV
H [§]	1.0 MeV - 20 MeV	750 keV - 60 MeV	He 17 MeV - 120 MeV*

§ If E triggers then H is not true

* Add to Dosimeter

Table 2. Pulse Height Comparator Boundaries

3.1.2.1.2. Counting Rate and Geometric Factor

The threshold flux for dielectric charging is about 2×10^6 electrons/cm²-sec and the maximum counting rate of solid state detector systems is of order 10⁵ /sec. The telescope should have some dynamic range above this minimum. Therefore, the aperture and solid angle of the telescope will result in a geometric factor of 1×10^{-3} cm²-ster to provide a dynamic range of 1000. The constraint on opening angle is

Bin	Electrons, MeV	Protons, MeV	Alphas, MeV
A	0.02 - 0.2	0.3 - 0.5	0.8 - 1.0
B	0.2 - 0.8		
C	>0.8		
D		0.5 - 4	1.0 - 5.0
E		4 - 12	120 >180
F		>12	
G			4 - 17
H			17 - 120

Table 3. Classification of Particles into Bins

that particles should not arrive so obliquely as to greatly increase their path length. We choose an opening half angle of 13.5° so that this increase is no greater than 4%.

The active area of the detector itself should be small to reduce background; a maximum of 0.25 cm^2 is acceptable, and areas as small as 0.01 cm^2 are desired.

3.1.2.2. Backgrounds

Unwanted particles can enter the detector through the front aperture or through the shielding on the sides. While active shielding operating in anti-coincidence with D1 and D2 can in principle eliminate side particles, we believe that passive shielding will suffice in this case because CEASE can tolerate a few high energy particles. A thickness of 8 g/cm^2 can probably best be achieved with tungsten (density 19.3, $Z = 74$) 0.42 cm thick. This corresponds to the range of 80 MeV protons and $> 10 \text{ MeV}$ electrons. The maximum flux of such particles is in the trapped radiation at the magnetic equator. Approximate maximum fluxes are:

Protons $> 100 \text{ MeV}$, $1 \times 10^4 / \text{cm}^2\text{-sec}$ Omnidirectional flux at $L = 1.5$

Electrons $> 4 \text{ MeV}$, $3 \times 10^3 / \text{cm}^2\text{-sec}$ Omnidirectional flux at $L = 4$

Assume that the detectors have active areas of 0.2 cm^2 and that the effective solid angle for a thin detector is about 2π , then the maximum rate is about $10^3 / \text{sec}$ from protons in the inner zone. This is lower than the counting rate due to lower energy particles coming through the front aperture.

Protons of energy $0.3 - 0.5 \text{ MeV}$ stop in D1 and will look like electrons, as seen in Table II. As protons do not effectively cause dielectric charging these are contaminating. The maximum flux of these protons is in the trapped radiation at the equator:

Protons $0.3 - 0.5 \text{ MeV}$, $1 \times 10^8 / \text{cm}^2\text{-sec}$ Omnidirectional flux at $L = 3$ to 4

Even from 1 steradian through the collimator, this exceeds the electron flux threshold for charging. However, in this same region of space there are higher-energy trapped protons that will be identified as such by the telescope. From the approximately known energy spectrum of trapped protons, the flux of $0.14 - 0.3 \text{ MeV}$ protons may be estimated for one L value and the corresponding D1

counting rate subtracted. The remainder would be the hazardous electrons with some residual contamination from protons. Thus, CEASE would tend to overwarn of electrons. While this procedure would not be acceptable in a scientific instrument, we believe that it is acceptable for CEASE.

3.2. Detector for Radiation Dose

Dose at a given site is defined as the energy deposited by ionizing particles per unit mass or volume. The rad unit is defined as 100 ergs per gram of material. The shielding between the site and the radiation in space determines the dose received. Dose results from the total mix of primary and secondary radiation that strikes the sensor.

3.2.1. Trade Studies on Various Sensors

We considered two types of sensor for total dose: MOS devices that experience a voltage shift related to total dose, and solid state detectors that transform absorbed energy to charge. Our report at the end of the first year describes some of the advantages of the MOS devices.

First, we will discuss the shielded solid state detector such as used in the CRRES Space Radiation Detector. It is a proven device and favored by Phillips Lab. We present an analysis and design of it, and then suggest a thermally controlled MOSFET as a possible device to carry in parallel with the solid-state detector design.

3.2.2. Adopted Sensor

The main dosimeter will use a single solid-state detector 400 μm thick behind a aluminum housing affording approximately 2π exposure to the radiation. Its shielding is representative of the minimum shielding that would be expected over PC boards on spacecraft. We have selected 0.06 inch Al = 0.41 g/cm^2 , corresponding to the range of 17 MeV protons. Figure 4 and Figure 5 are the cross section of two possible dosimeters. The hemispherical dome shields the detector uniformly over 2π steradians. However, the planar shield more closely mimics the geometry of a typical rectangular equipment box on a spacecraft. It is also somewhat easier to build. We recommend the planar geometry.

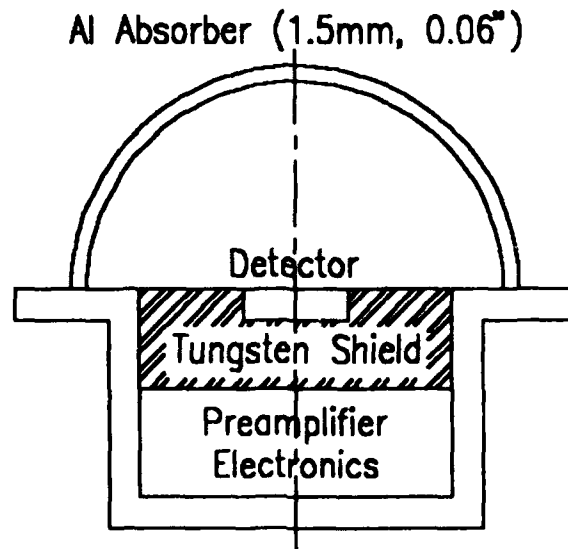


Figure 4. Hemispherical Dosimeter Cross Section

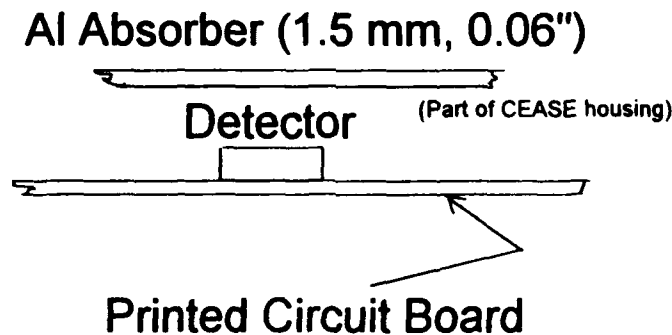


Figure 5. Planar Dosimeter

As an ancillary radiation sensor, second detector D2 of the coincidence telescope will function as a dosimeter behind the shielding afforded by the telescope absorber and D1. This amounts to $34,900 \mu\text{g}/\text{cm}^2$ of Si, the range of ~ 3 MeV protons.

3.2.2.1. Response

3.2.2.1.1. Energy

Figure 2 shows the response of D2 in the coincidence telescope. Figure 6 shows the response of a 400 μm thick detector to electrons, protons, and alpha particles. The absorber is 0.060 inch thick (0.41 g/cm^2). The figure shows Bins I to IV, defined entirely by energy loss in the single detector. Particles may enter the dosimeter detector obliquely thus having a longer path length through it. Figure 7 shows the response to particles entering at 60° from the normal; their path length is 800 μm .

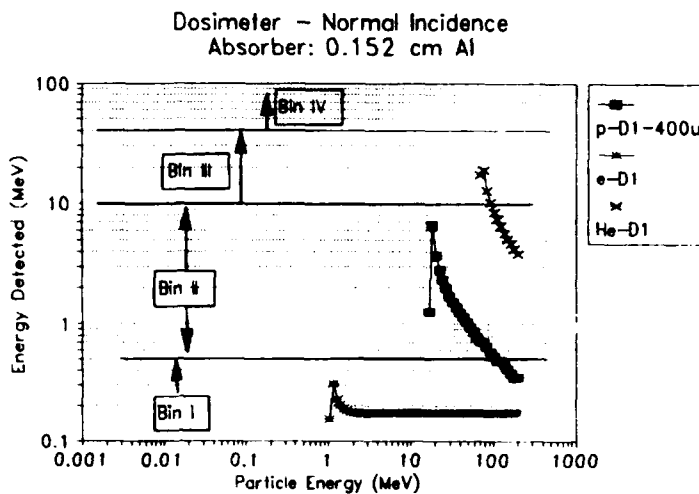


Figure 6. Dosimeter Response to Normal Incidence

Table 4 is the response of the dosimeters. In determining what particles produce responses in the various bins we ignore the very narrow energy range of protons and alphas that stop in the detector with energy loss in the Bin I and are not distinguishable from electrons. Only particles

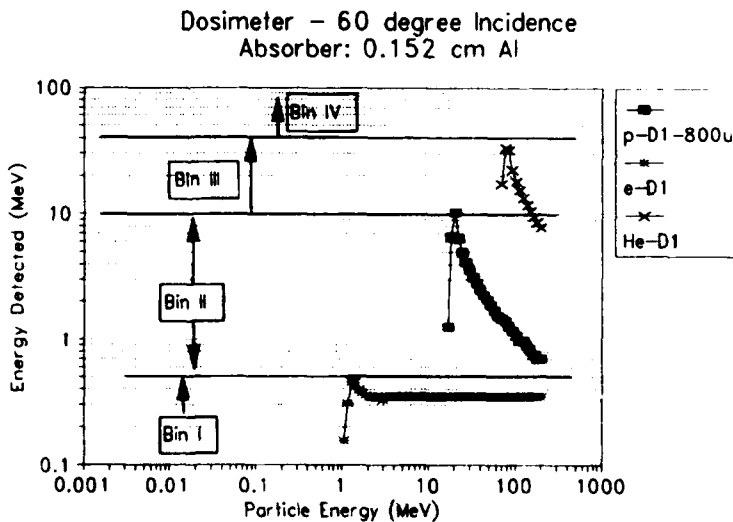


Figure 7. Dosimeter Response to 60° Incidence

with $Z > 2$ (or nuclear interactions that result in particles with $Z > 2$) can trigger events in Bin IV.

3.2.2.1.2. Counting Rate and Geometric Factor

Bin	Electrons	Protons	Alphas
All D2	> 0.2 MeV	> 4 MeV	> 17 MeV
I	1 - > 10	> 100	
II		18 - 100	100 - > 1000
III			70 - 120
IV	$Z > 2$ and nuclear interactions		

Table 4. Dosimeter Response

The highest flux of particles that will penetrate the dosimeter shield is trapped electrons.

Electrons ~ 1
MeV, 3×10^6
/cm²-sec
Omnidirectional
flux at $L = 4$

In order to keep the counting rate below 10^5 /sec due to particles

approaching from a hemisphere, the detector area should be $< 0.1 \text{ cm}^2$.

3.2.2.2. Backgrounds

There is no background for a dosimeter other than any local radioisotope in the detector. The sensitive element should be shielded in a way that is characteristic of the location of sensitive components on a host spacecraft. The 0.41 g/cm^2 in front and 8 g/cm^2 behind the sensor mimic the surroundings of a circuit board component just under an aluminum cover 0.060 inch thick and having the thickness of a spacecraft behind it ($\sim 3 \text{ cm}$).

3.3. Temperature Controlled MOSFET Dosimeter

MOSFET dosimeters have been used extensively in space to monitor total radiation dose. These devices have the great advantage that they directly integrate dose within the device, over the full dynamic range, and thus provide accurate measurements independent of spectrum without requiring the use of analog to digital conversion and integration. However, results from these

sensors have not been dependable due to temperature effects. At elevated temperature, the annealing rate of the MOSFET becomes significant, corrupting the data of the dosimeter. Additionally, the calibration of the MOSFET device is temperature dependent. For a MOSFET dosimeter to provide reliable data, it should be operated at a constant temperature throughout the flight.

As an alternative, or even redundant method of measuring total radiation dose we have investigated the use of a MOSFET device placed on a Peltier cooler/heater. A temperature sensor in combination with a closed-loop controller would maintain temperature at a constant 20°C, heating or cooling as necessary.

This device would be assembled in a small TO-8 hybrid package. The controller and monitor circuitry would add an additional 200 mW of power to the CEASE power budget.

TEMPERATURE CONTROLLED MOSFET DOSIMETER

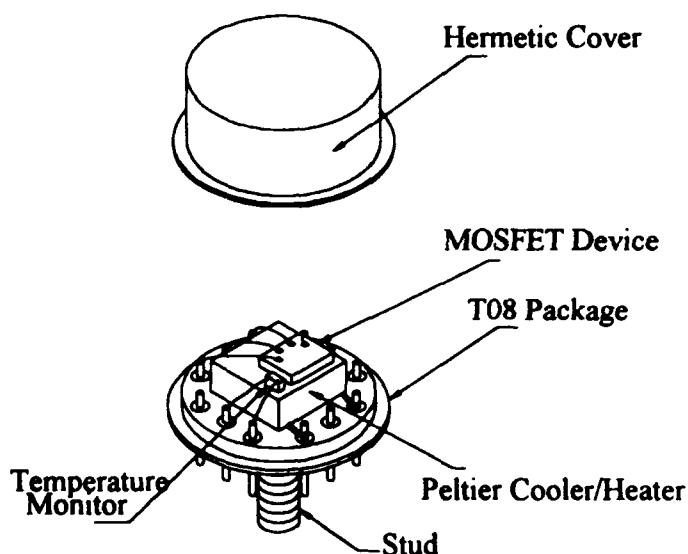


Figure 8. Hybrid MOSFET Dosimeter with Thermal Control

We have concluded that the inclusion of such a device is quite feasible, and would enhance the performance of CEASE. Figure 8 depicts the hybrid MOSFET dosimeter.

4. Warning Flags

4.1. Sensor Input to Warning Logic

Table 5 lists the outputs of the detectors, which are input to the warning algorithms. Software and firmware will produce the warning flags from the detector outputs. The count rates in Table 4 are averaged over 100 sec intervals. Thus, Table 5 uses conversion coefficients. The set appropriate for the detectors discussed above is:

G_1 = geometric factor of telescope: $0.001 \text{ cm}^2\text{-steradian}$.

M_{D2} = mass of D2: 8.1×10^{-3} grams.

M_{Dose} = mass of dosimeter: 1.1×10^{-2} grams.

$V_{bit}/V_{dos} = 2.5 \times 10^{-7}$ assuming detector volume is $0.1 \text{ cm}^2 \times 400 \text{ } \mu\text{m}$ and device volume is $10 \text{ } \mu\text{m}$ cubed. For smaller devices the coefficient could be 1000 times smaller.

Knowledge of these factors will change and improve as detailed design advances.

Anomaly	[Output #] Bins	Comment
Surface Dielectric Charging	[1] A - (D + E), count rate	Flux = count rate/ G_1
Deep Dielectric Charging	[2] B + C, count rate	Flux = count rate/ G_1
Total Radiation Dose: Behind 0.035 g/cm^2	[3] Sum D2 pulse ht, MeV	Dose = (MeV) / ($6.25 \times 10^7 \times M_{D2}$)
Total Radiation Dose: Behind 0.41 g/cm^2	[4] Sum (I-IV) pulse ht, MeV	Dose = (MeV) / ($6.25 \times 10^7 \times M_{Dose}$)
SEU	[5] IV, count rate	SEU/bit-day = $V_{bit}/V_{Dose} \times$ count rate $\times 86,400 \text{ sec/day}$

Table 5. Outputs from Detectors to Warning Algorithms Logic

4.2. Warning Algorithms

Charging anomalies result from effects that accumulate at a sufficiently high rate. Therefore, both counting rate and accumulated count are important. The threshold fluence is the integral of flux while the flux exceeds its critical threshold. During periods of low flux, the accumulated charge in a dielectric will relax so that significant fluence will again accumulate when the flux exceeds the threshold value. The relaxation time depends upon the dielectric resistivity and ranges up to many hours.

Total dose is cumulative, mostly independent of dose rate. Some healing does occur, partly depending on temperature. SEU are not cumulative so only rate is significant.

Table 6 incorporates the critical physical values and reflects the above facts.

Quantity	Critical Values	Base Level
Flux: Count rate Outputs 1	2×10^6 flux = 2×10^3 counts/sec	1×10^2 /sec
Flux: Count rate Outputs 2	2×10^6 flux = 2×10^3 counts/sec	1×10^2 /sec
Fluence: Total Count = integral of rate 1 > 10^3 /sec in past 10^4 sec	5×10^{11} fluence = 5×10^8 counts	1×10^7 counts
Fluence: Total Count = integral of rate 2 > 10^3 /sec in past 10^4 sec	5×10^{11} fluence = 5×10^8 counts	1×10^7 counts
Dose: Sum pulse heights; Output 3	10 krad = 7.7×10^{13} MeV in D2	1×10^{13} MeV
Dose: Sum pulse heights; Output 4	10 krad = 5.7×10^{13} MeV in dosimeter	1×10^{13} MeV
SEU rate: Count rate Output 5	1×10^{-3} SEU/bit-day = 2.2×10^{-5} counts/sec	1×10^{-5} /sec

Table 6. Critical and Base Values

For each of the seven quantity in Table 6 we define 8 warning levels, 0,1,2...7 corresponding to 1,3,10...3000 times the base level. (The level is thus $2 \times \log(\text{quantity}/\text{base.})$) Define a warning for each of the two kinds of charging that combines flux and fluence; this combined level equals one-half the sum of the rate plus the total count warning levels.

This scheme provides eight warning levels for each of five anomalies. The levels that trigger flags can be selected for a particular application. A general example would be:

- ♦ -Level 0 to 2: Some hazard
- ♦ -Level 3 to 5: Moderate hazard
- ♦ -Level 6 to 7; Extreme hazard

4.3. Comments

In general the dose registered in D2 is less significant than in the dosimeter because most sensitive devices are behind at least 0.060 inch shielding.

It would be possible to respond to both the rate of dose buildup as well as the accumulated dose in the same manner as done for flux and fluence that cause dielectric charging. The difference would be that there is no minimum dose rate or maximum accumulation time for dosage. The CEASE CPU will maintain flux and fluence data that may be transferred to the host if interrogated.

Measuring low energy electron fluxes from 5 to 20 keV in an unambiguous manner may be important. We can extend our laboratory measurements to this regime using solid-state detectors, however the CEASE environment will not be the generally benign state found in a laboratory. We use particularly sensitive and quiet solid-state detectors, and by carefully lowering the amplifier threshold we can resolve 5 keV. Attempting this in space with the CEASE instrument would be hazardous. The cumulative effects of radiation damage and possible higher temperature operation could raise the solid state device noise ceiling to levels well above such a low threshold. If this occurred, the CEASE would begin raising false charging alerts.

We believe that a very simple electrostatic analyzer tuned to this narrow band of interest (5 to 25 keV electrons) and using a Channel Electron Multiplier

can provide this data. Such a device would not significantly increase the size, power, or complexity of the CEASE instrument.

5. IV Hardware Implementation

5.1. Signal Processing Electronics

The function of the signal processing electronics is to linearly amplify signals generated by particles in the detectors, to filter these signals for maximum signal to noise ratio, and to separate them by height for digital analysis. In addition to minimum noise, this circuitry must meet the requirements of adequate dynamic range, reasonable insensitivity to count rate variation over the expected ranges of input particle flux, and low power. These considerations apply equally to the CEASE telescope and dosimeter, so the electronics for both will be discussed together.

The conventional approach to designing analog signal processing electronics for space flight instrumentation is to use discrete parts and integrated circuits to build the required functions. A refinement which improves performance and power and space efficiency is to hybridize portions of the circuit. An alternate approach in use for the past few years is to develop an application-specific integrated circuit which incorporates as much of the required circuitry as possible. This has been made feasible by the development of rad-hard analog CMOS technology. We have investigated the use of this technology in CEASE as a means of power, mass and volume reduction. Our conclusion is that the development of a CEASE ASIC is possible, but at the present time the advantages do not justify the high cost and a much greater (and less predictable) development time. Using conventional technology, the CEASE design will still greatly improve on our initial estimates of required power, weight and volume.

The following sections briefly describe the elements of the analog signal processing chains.

5.1.1. Charge Sensitive Preamplifier

The charge-sensitive preamplifier is the first element in the amplification chain and is thus the critical component in achieving low noise performance. The most suitable amplifier available for this application is the Amptek A250, which will be used for all three detectors. Figure 9 shows the configurations of the charge amplifiers with detectors.

5.1.2. Shaping amplifiers and gain stages

Shaping, or filtering, of the tail pulse outputs from the preamps is critical to obtaining the combination of wide dynamic range and high count rates required of the telescope electronics. Neglecting $Z > 2$ and star events, the energy dynamic range of the telescope signals is approximately 1000, and the permissible dead time is 2 μ s. To meet these requirements, 5-pole shaping with pulse width of 400 ns will be used, implemented with A275 amplifiers with passive shaping. The highest two energy channels will be derived from the amplifier chain prior to the final shaping stage and will thus use three pole shaping instead of 5. The amplifier chains are shown in Figures 10, 11, and 12.

5.1.3. Stacked discriminators

The conversion of pulse height information to digital form may be performed with A/D converters or with a set of comparators (stacked discriminators), separating pulses into bins. The A/D approach is useful when a large number of bins are required and/or the energy dynamic range is limited. For the CEASE analysis, the required number of bins is small and dynamic range large, so that stacked discriminators are the more efficient approach. A150 pulse height discriminators will be used, with discrimination thresholds set between 0.1 and 3V.

5.1.4. Dose Integrator Circuit

Dose measurement requires the integration of all energy deposited in the detector from events over some threshold in energy. The MOS dosimeter is an example of a class of dosimeters in which integration of total dose occurs within the detector element itself. The use of a silicon detector requires that the electronics perform the integration. This is usually achieved in spaceflight dosimeters by using some type of A/D conversion to convert energy deposited in an event to digital form and summing these events with a microprocessor. To meet the requirements of compactness and low power, we have divided the dosimeter output into 4 bins and the telescope output into 3 bins. Each bin must

be assigned an energy weight, which is the mean energy loss for all particles within that bin. The determination of these weights is dependent on assumptions made about input particle spectra and angular distributions.

An alternative approach to dose integration which is independent of these assumptions is to perform the integration directly on the shaped analog pulses, using an analog integrator. The result is a much more accurate measurement of dose. With this technique, the integrator is gated on for each pulse which exceeds a low-level threshold, and the output continues to rise until a fixed threshold is reached, corresponding to a known increment of total dose. At this time, the integrator is reset and a counter incremented to record the accumulation of this dose increment. This technique would permit very high count rates, which would allow a larger detector and thus better SEU statistics to be achieved. It would also remove the requirement for three of the four dosimeter bins previously described. We intend to breadboard an analog integrator to determine its suitability for use with both the dosimeter and the D2 output. See Figure 13.

5.2. Power Supplies

Amptek will design and construct a custom resonant DC-to-DC converter to power the CEASE electronics. The design will be similar to supplies that we build for the SSJ/4 and SSJ/5 instruments on the DMSP satellites. This design has been flown many times and has been extremely reliable. It is very efficient, compact, quiet, and can regulate over a wide range of input voltages. Its reliability, efficiency, and versatility make it an ideal candidate for the CEASE.

Using such a resonant converter allows us to customize the number and type of transformer output windings. Thus the addition of an electrostatic analyzer to provide additional low-energy electron data would not impact our size or power by very much. We believe that we can still achieve the envelope, weight, and power presented in this report.

One other aspect of the CEASE power supply is a need to have a keep-alive power line from our host spacecraft, or alternatively carry a small battery to maintain our memory if the CEASE loses power.

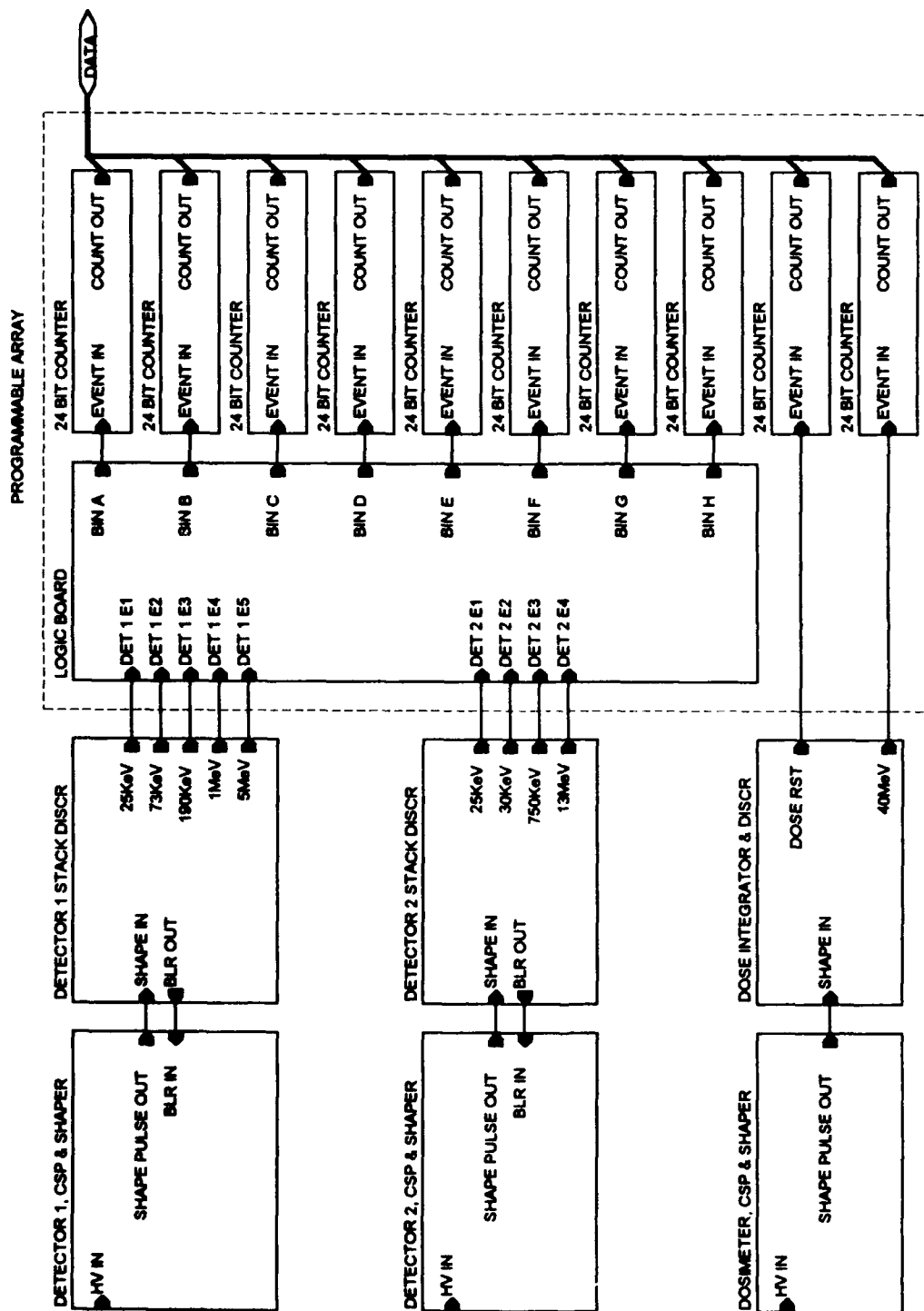


Figure 9 - CEASE Front End Electronics Block Diagram

NOTES:

1. R8 & R9 WILL BE DIFFERENT FOR D1, D2 & DOSIMETER.

2. BRL IS NOT USED ON THE DOSIMETER CSP.

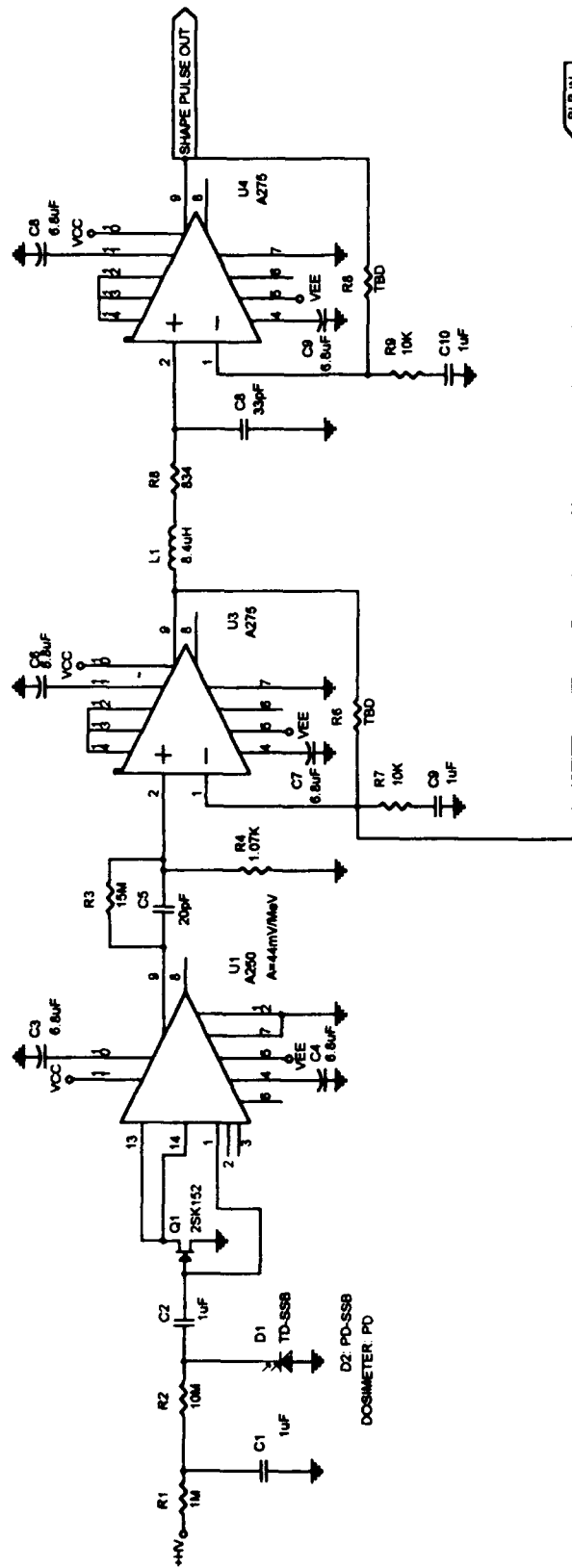
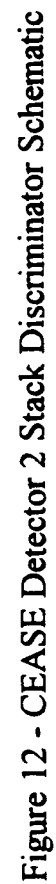


Figure 10- D1, D2, and Dosimeter CSP & Shaper Schematic



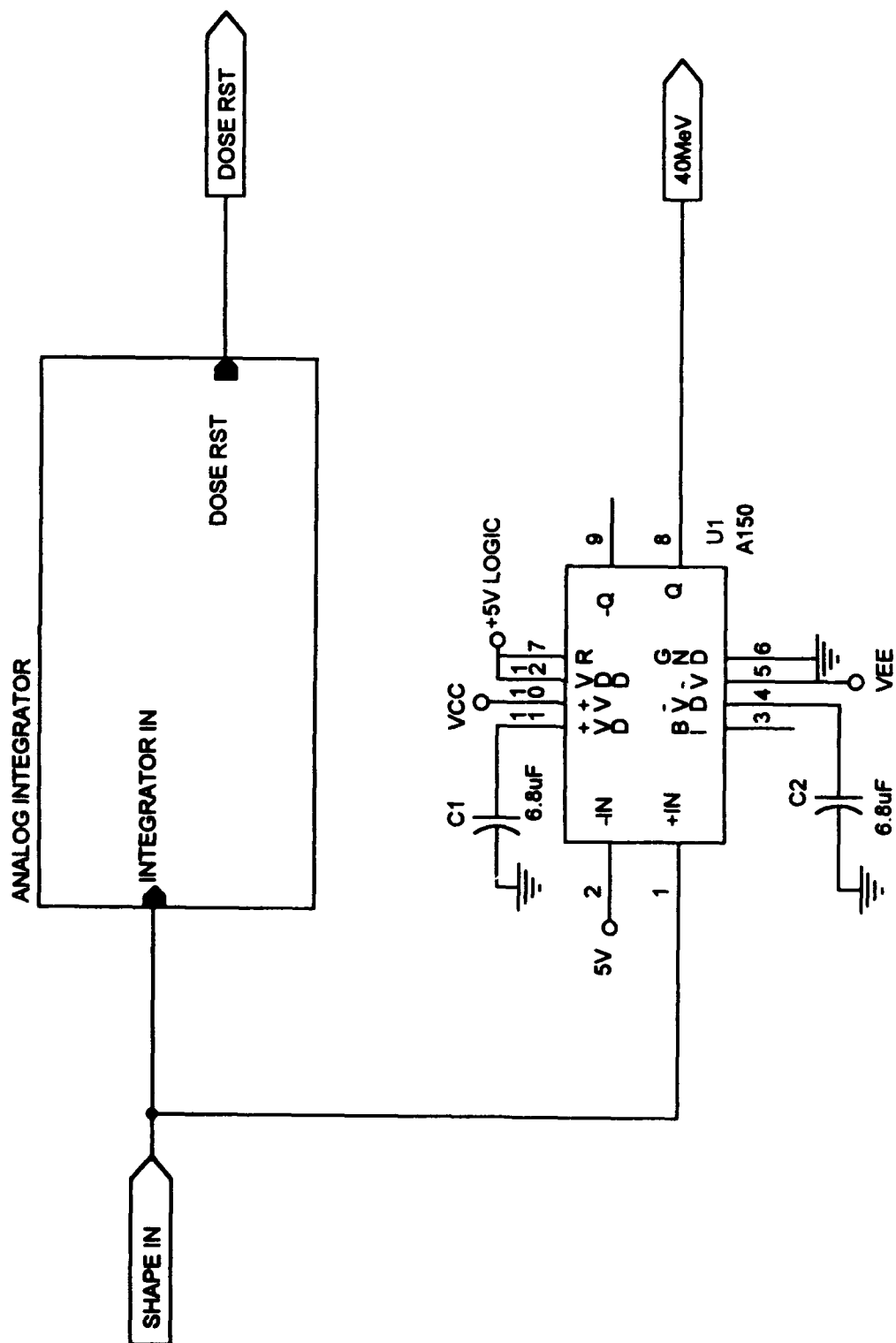


Figure 13 - CEASE Dose Integrator & Discriminator

5.3. Overview of CEASE Control Electronics

The CEASE control electronics is a microprocessor-based system that is responsible for analyzing sensor data to determine the existence of various radiation conditions. The sensor inputs to the control electronics are from the telescope, the dosimeter, and (optionally) the ESA. (Refer to Figure 15.).

The outputs of the two detectors in the telescope feed through amplifier chains into a series of stacked discriminators, which feed into a gate array. The gate array contains logic to coincidence the pulses from the two detectors and to separate the pulses into 8 bins depending on the energy deposited in each detector (See Table 3). These 8 bins are implemented as 20-bit counters in the gate array.

The output of the dosimeter feeds through both a discriminator and an analog integrator into the gate array. The pulses from the discriminator are placed in the SEU bin, and the pulses from the analog integrator are placed in the total dose bin.

The ten bins in the gate array are read periodically by the microprocessor. The processor accumulates these bins over time, where appropriate, and feeds the resulting accumulations through the various warning algorithms. The output of these algorithms is then passed on to the spacecraft, either through discrete warning flags, or through a serial data interface.

The processor uses its idle time to protect the memory from SEUs by storing data blocks in multiple places with independent checksums. It also obtains extra SEU information by sweeping unused memory blocks for SEUs.

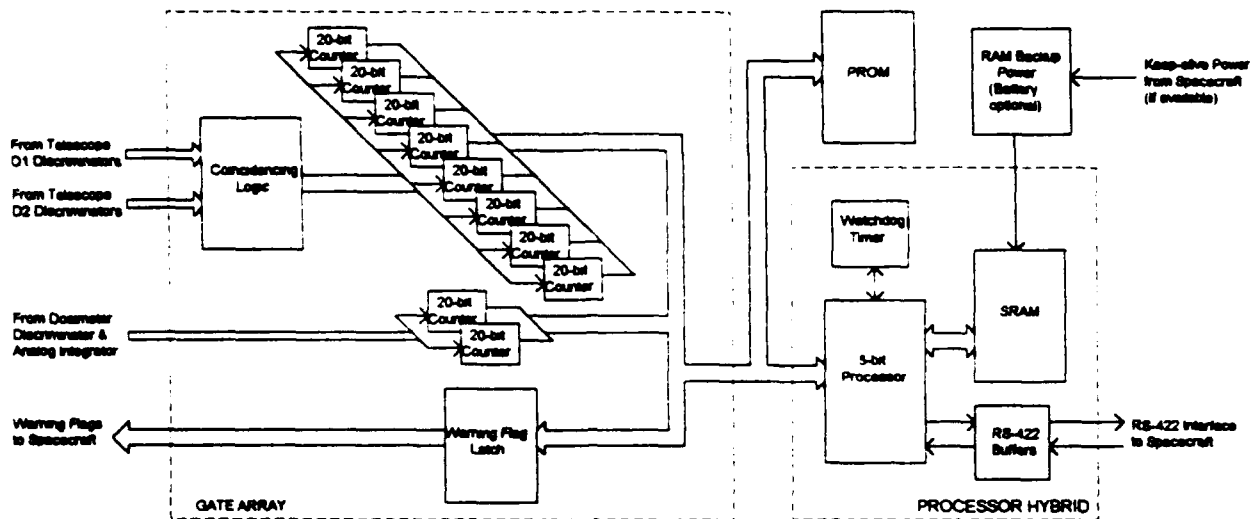


Figure 15. CEASE CPU Block Diagram

5.3.1. CPU Configuration

The proposed processor design for CEASE employs several techniques to achieve compact size and very low operating power. The first involves hybridizing the processor and a number of support ICs. The other recommended technique is the use of a gate array. The use of these two technologies allows the entire CPU to exist on a single 3.75 inch x 3.75 inch PC board. See Figure 14.

5.3.1.1. Hybrid Processor

The processor hybrid would likely be composed of the following:

- HS80C85 processor
- UT67164 8Kx8 SRAM
- RS-422 driver and receiver
- 54AC373 address latch
- 54AC138 address decoder
- Watchdog timer
- Level-shifter for battery-backed RAM

The hybrid could be constructed with a layer of radiation shielding material, such as tungsten, which could improve the total dose tolerated by the shielded components by as much as several hundred times. As all components are tolerant to at least 100 krad, this may not be necessary, but it is available if 100 krad tolerance is deemed inadequate.

These devices are described in the following sections.

5.3.1.2. Microprocessor

The HS80C85 microprocessor is suggested because of its flight heritage, very low power consumption, 100 krad processing, and the availability of a significant quantity of development tools. Also, because it has a simple 8-bit interface and a minimum of extraneous functions, it requires fewer support chips and is more compact than other radiation-hardened processors. (i.e., HS80C86, UT1750, etc.)

A less desirable alternative to using a microprocessor would be to integrate the required functionality of the processor into a gate array. While it would be possible to reduce the entire CEASE control system to one gate array with one or two support chips, the major disadvantage to this concept is the loss of flexibility. The use of a processor allows changing telemetry formats, warning flag configurations, and thresholds. To make these changes with a gate array would mandate redesign, simulation, etc.

5.3.1.3. Memory

Not only does the processor need general-purpose RAM to maintain and process the sensor data set, but the desire to accumulate total dose over the life of the instrument requires some means to maintain that measurement through power interruptions. The UT67164 SRAM is recommended because of its very low data retention power, excellent SEU characteristics, and 1 Mrad processing.

Two types of backup power are provided for in this design. The preferable option is the use of keep-alive power from the spacecraft to maintain the SRAM. If this is not available, then a battery can be used. To extend battery life, the battery will remain disconnected until an arming plug is installed shortly before launch.

An better alternative to using a battery would be to add a non-volatile memory such as an EEPROM to the hybrid. Unfortunately, no EEPROMs with appropriate radiation tolerance have been located. While this technology cannot be recommended at this time, it might be possible to design the hybrid to take advantage of such a part when a radiation tolerant version becomes available.

5.3.1.4. RS-422 Interface

For spacecraft that require detailed anomaly information, or have telemetry available for the CEASE instrument, an RS-422 asynchronous serial interface is

provided. While other interfaces could be implemented, the RS-422 interface requires a minimum of hardware and software overhead. In addition, RS-422 is becoming a standard on newer spacecraft.

To make the interface more flexible, logic will be included in the gate array to support synchronous RS-422 in addition to asynchronous RS-422. The interface can be jumpered to operate at any standard baud rate for asynchronous use, or use an external clock for synchronous use.

This interface is bi-directional, which allows the spacecraft to send commands to CEASE. Possible commands might be 'Send extended telemetry packet', 'Reset total dose counter', 'Prepare for power-down', etc.

5.3.1.5. Miscellaneous

In addition to the processor, RAM and RS-422 interface, the processor hybrid will contain a watchdog timer, processor support logic, and logic to support the battery-backed RAM.

The watchdog timer will allow the processor to recover from execution failures caused by SEUs or other anomalies. Because the RAM maintains its contents through resets and power interruptions and because critical data will be stored in multiple locations with independent checksums, the processor should be able to fully recover from an unexpected fault.

The processor support logic, which is an address latch and an address decoder, will incorporate NSC FACT logic which is radiation tolerant in excess of 100 krad. The RAM backup-power logic, which is used to convert logic signals to the backup supply voltage, will consist of Harris CD4000-family logic which is available radiation-hardened to 1 Mrad.

5.3.2. Gate Array

The bulk of the logic for the CPU will be contained in the gate array. It will include ten 20-bit counters, the detector coincidencing logic for the telescope, the baud rate generator and control logic for the RS-422 interface, the system timer, and counters and control logic for the ESA (if applicable). Field-programmable technology for the gate array is preferable because it allows more flexibility in adapting the instrument to meet the needs of a particular spacecraft. (See Figure 16.)

The coincidencing logic is an important part of the gate array. It compensates for skew in pulse arrival times from the stacked discriminators by latching each pulse separately, and then synchronously incrementing the appropriate bins by

gating detector 1 pulses with detector 2 pulses. Also, since the stacked discriminators generate pulses in all output channels of amplitude less than or equal to the input pulse amplitude, the logic chooses only the highest amplitude pulse to coincidence.

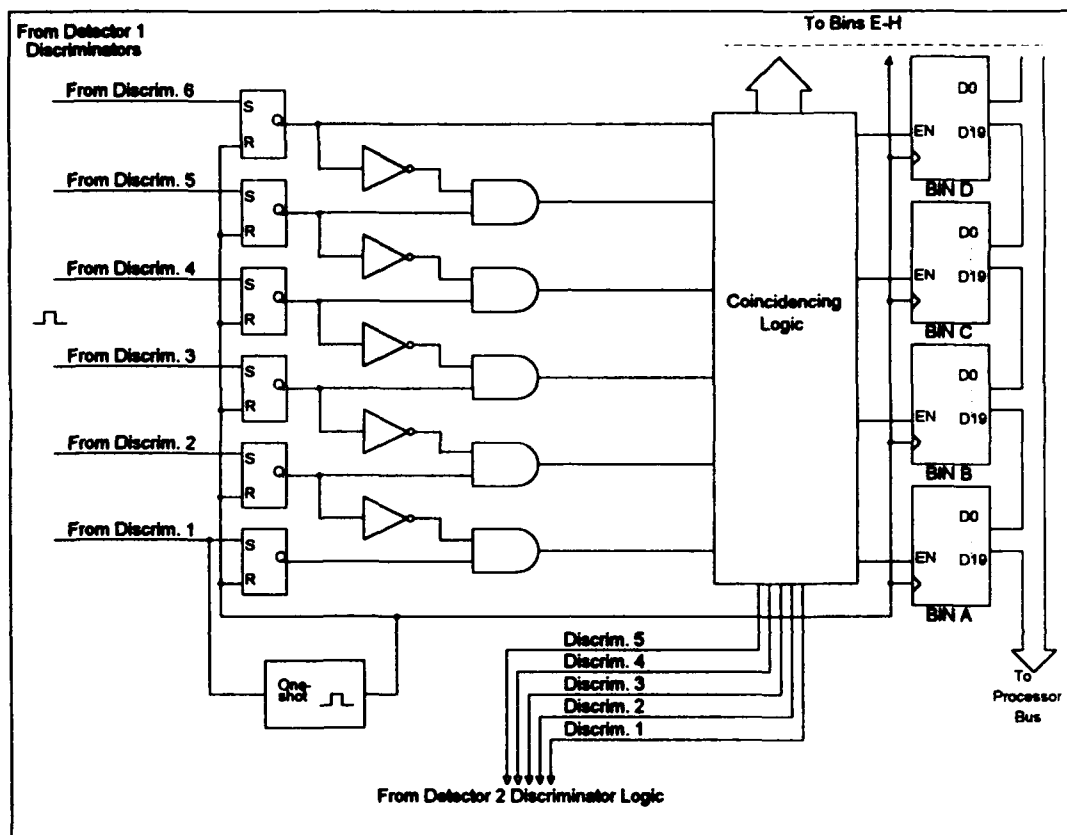


Figure 16. Gate array coinciding logic.

The preferred gate array is the Actel A1280 FPGA, because of its low power, good radiation tolerance, high gate count, and relatively low development cost. GEC Plessey, United Technologies and others make mask-programmed radiation-hardened gate arrays which could be used if difficulties were to arise with the FPGA implementation.

The use of hybrids was also considered for implementing the counters and coinciding logic, but they limit flexibility and do not achieve the extremely high density of the gate array.

5.3.3. Telemetry

There are two methods of communication between CEASE and the spacecraft. The first is the use of discrete warning flags. The other is the use of the RS-422 serial channel.

CEASE generates warning flags for four anomalies each of which can be divided into up to eight warning levels. Thus, there are 12 discretes which would nominally be divided into four 3-bit flags. However, these are configurable by software to make the flags more easily compatible with the spacecraft's discrete telemetry system.

The extended telemetry will include total dose measured to date and the time over which this measurement was accumulated, the current dose rate, current SEU rate and other TBD data. It will nominally be available by request from the spacecraft. Optionally, it could be sent to the spacecraft periodically.

6. Software

The CEASE control software is responsible for managing the sensor data, processing the warning algorithms to determine warning levels, formatting extended telemetry where applicable, maintaining checksums for key data areas, and sweeping the RAM for SEUs. The software will be written in a modular format, such that the telemetry module and the warning flag module can be modified without impacting the rest of the software.

7. CEASE Specifications (weight, power, and envelope)

The CEASE instrument presented above is a very simple device. It consists of a solid state telescope and a pair of dosimeters. Since accurate detailed measurements are not necessary for this mission, the electronics are reduced to the bare essentials. Even if an electrostatic analyzer were added to measure low energy electron fluxes that can not be unambiguously resolved in the solid state telescope, the additional hardware and circuitry would not particularly impact the size, weight, or power requirements for the CEASE. Please see Figure 17.

- ◆ We estimate power dissipation for the CEASE to be 2 watts or less.
- ◆ We estimate the CEASE weight to be 2 pounds or less.

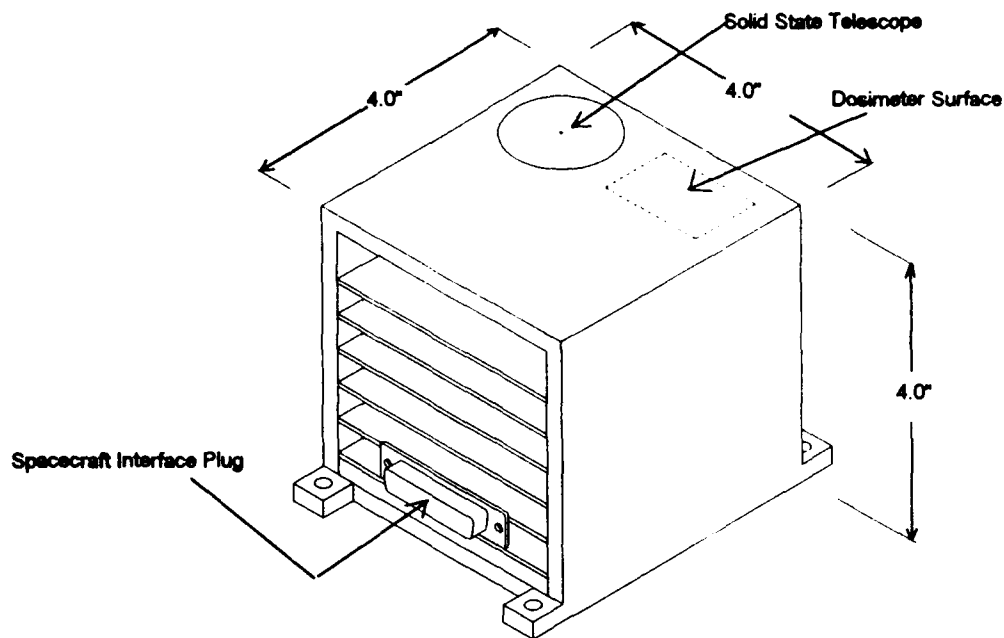


Figure 17. Anticipated CEASE Envelope.

The package is symmetrical four inches on a side. This symmetry allows mounting the detectors and the mounting feet in any orientation with respect to each other. Thus the instrument may be configured to view from any plane with respect to its mounting feet. We believe that this increases its versatility.

The Interface plug is depicted as a 25 pin "D" connector. We will include on this plug the spacecraft power and keep alive power (if available), twelve hazard alert bi-levels, and a 4 to 9 wire RS-422 interface.

8. Proposed Development Schedule

Amptek believes that the environmental knowledge gained from the CRRES satellite combined with the designs presented in this report define the necessary characteristics of the CEASE instrument. The technology to build this instrument is presently available. Amptek therefore recommends that the next phase of the CEASE program be the complete design, construction, and testing of a proto-flight model of the CEASE. We believe that this would be the most cost effective method of demonstrating the CEASE principle of anomaly forecasting and its value to operational satellites. An accelerated funding of this project can produce a flight unit in two years rather than the originally planned "brass board" system that was scheduled in three years.

The attached schedule (Figure 18) is prepared with this two year proto-flight unit development as its goal. Since CEASE is intended to be a generic space flight instrument, no specific spacecraft or mission is proposed, but rather the demonstration of adapting to a variety of carriers and environments. If a particular mission were targeted, the materials presented here could serve as part of that mission's PDR.

[illegible]

37

This page intentionally left blank

Appendix I. Response Curves for Various Telescope Parameters

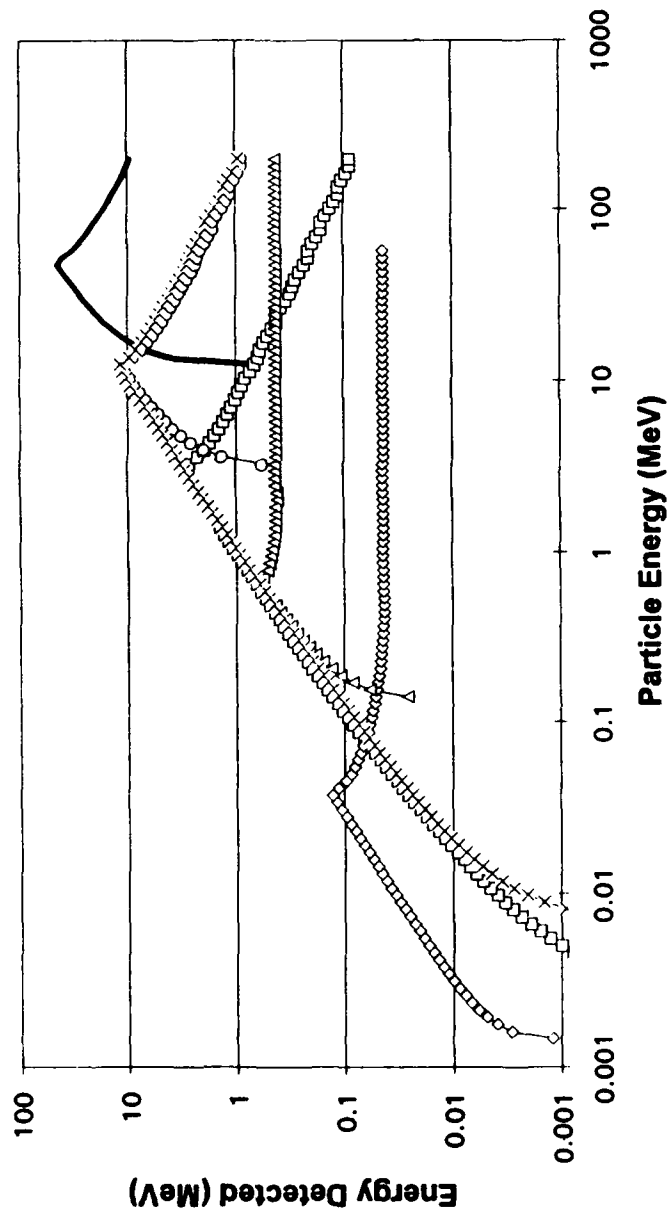
There follows a representative set of response curves of a two element (D1 and D2) solid state telescope preceded by an absorber. Detector D1 has a front dead layer $34.5 \mu\text{g}/\text{cm}^2$ thick, and between D1 and D2 is a $46.5 \mu\text{g}/\text{cm}^2$ dead layer. We made calculations with the following parameters:

RUN	Abs: $\mu\text{g}/\text{cm}^2$	D1: μm , ($\mu\text{g}/\text{cm}^2$)	D2: μm , ($\mu\text{g}/\text{cm}^2$)
1	0 - 1200	100 (23,000)	1000, (230,000)
2	0 - 1100	150 (34,500)	1000, (230,000)
3	0 - 1000	200 (46,000)	1000
4	0 - 1000	400 (92,000)	1000
5	0 - 1000 and 10,000	1000 (230,000)	100

The figures are labeled with the values. We used standard range energy tables. Electrons will be less accurate than the proton curves because of scattering.

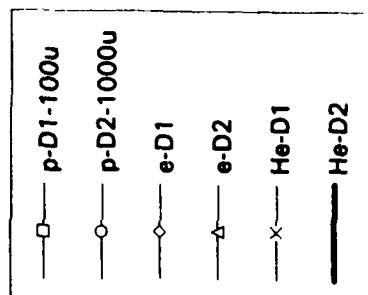
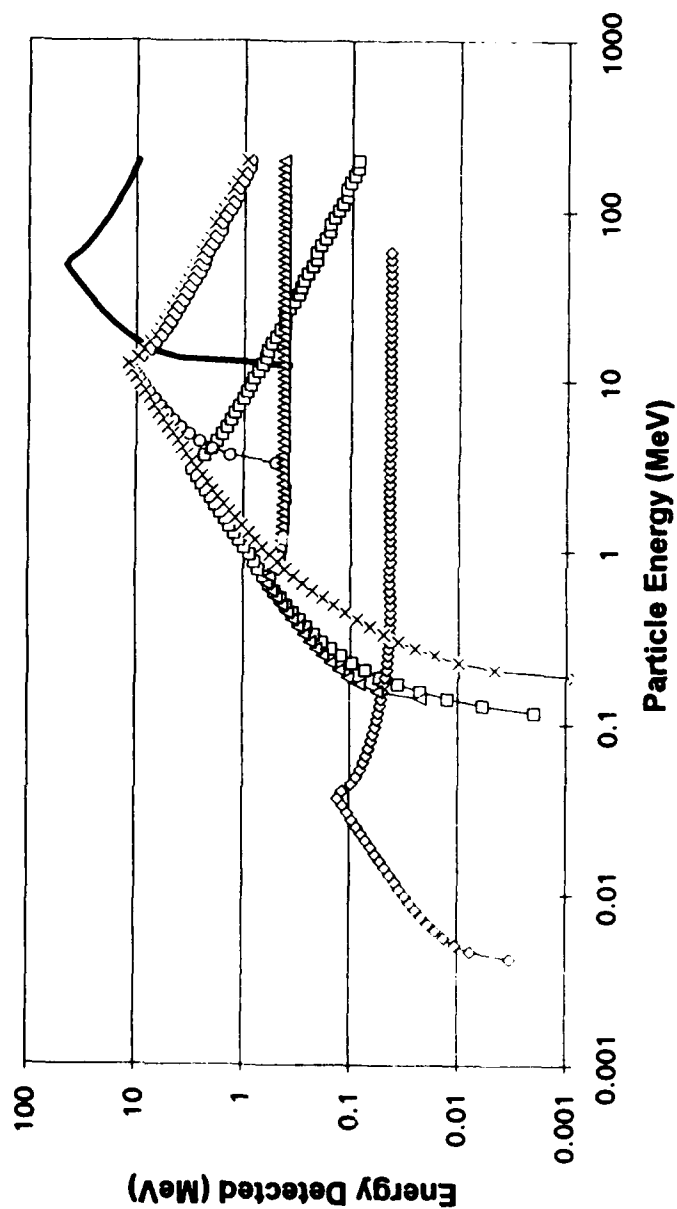
From these curves we selected values for the design that is presented in the body of this report.

Absorber: 0 ug/cm² Al
 Front Detector: 34.5 ug/cm² Si(Dead Layer)/
 23 mg/cm² Si(D1)/46 ug/cm² Si(Dead Layer)



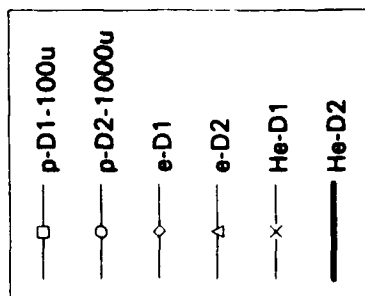
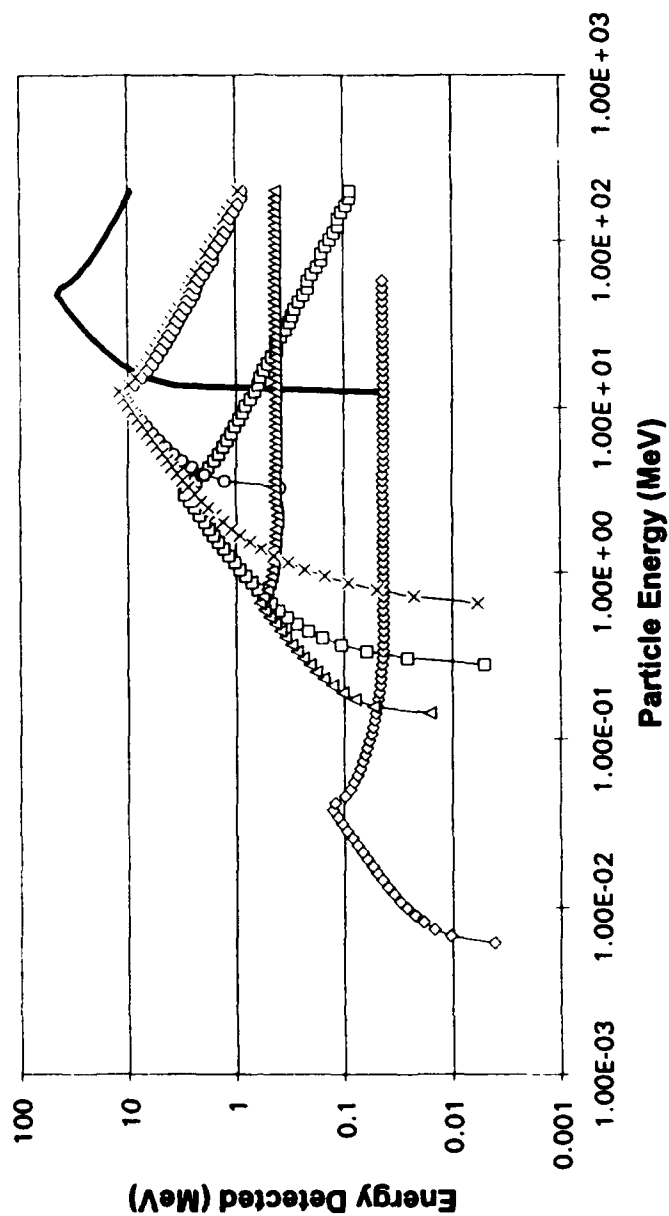
Run 1, 00, 100, 1000

Absorber: 300 ug/cm² Al
Front Detector: 34.5 ug/cm² Si(Dead Layer)/
23 mg/cm² Si(D1)/46 ug/cm² Si(Dead Layer)



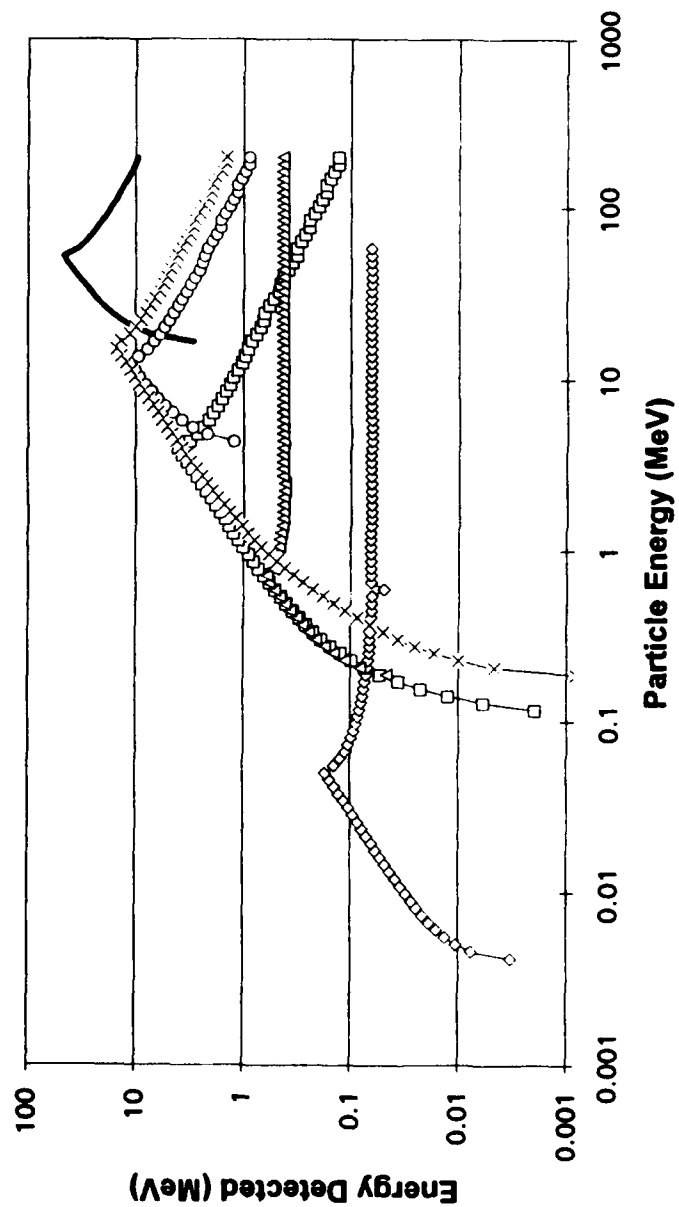
Run 1, 300, 100, 1000

Absorber: 700 ug/cm² Al
 Front Detector: 34.5 ug/cm² Si(Dead Layer)/
 23 mg/cm² Si(D1)/46 ug/cm² Si(Dead Layer)



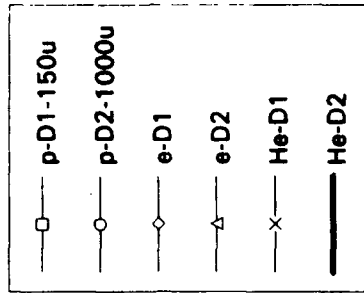
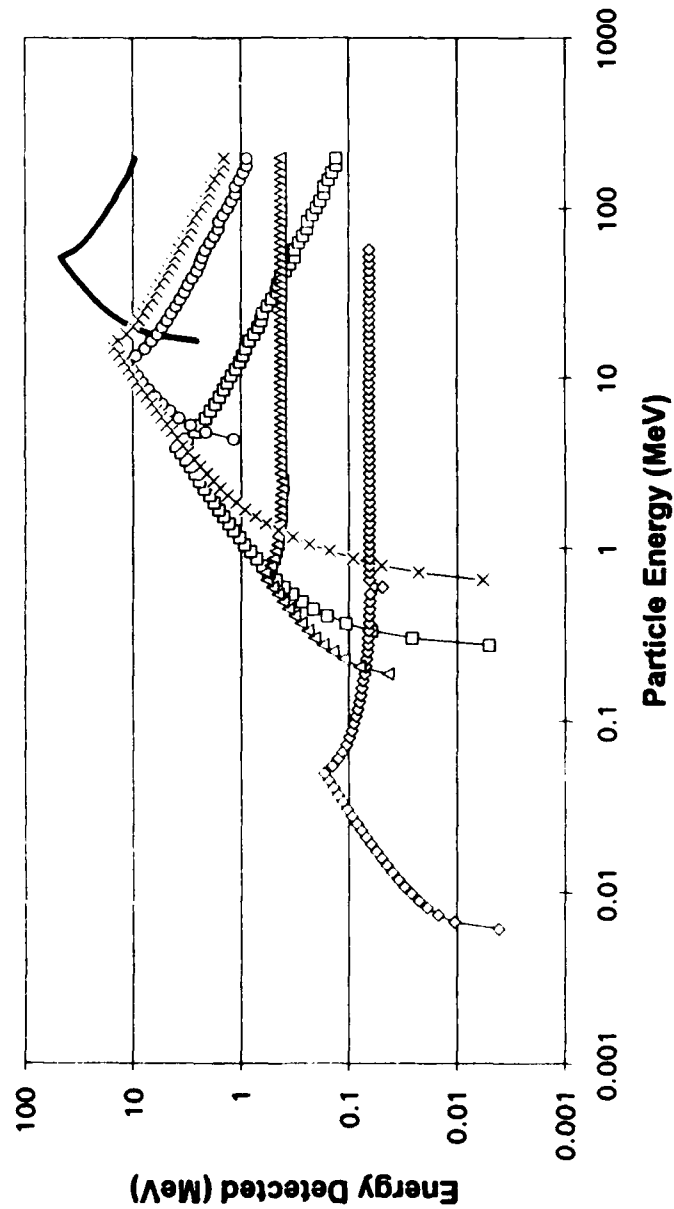
Run 1, 700, 100, 1000

Absorber: 300 ug/cm² Al
Front Detector: 34.5 ug/cm² Si(Dead Layer)/
34.5 mg/cm² Si(D1)/46 ug/cm² Si(Dead Layer)



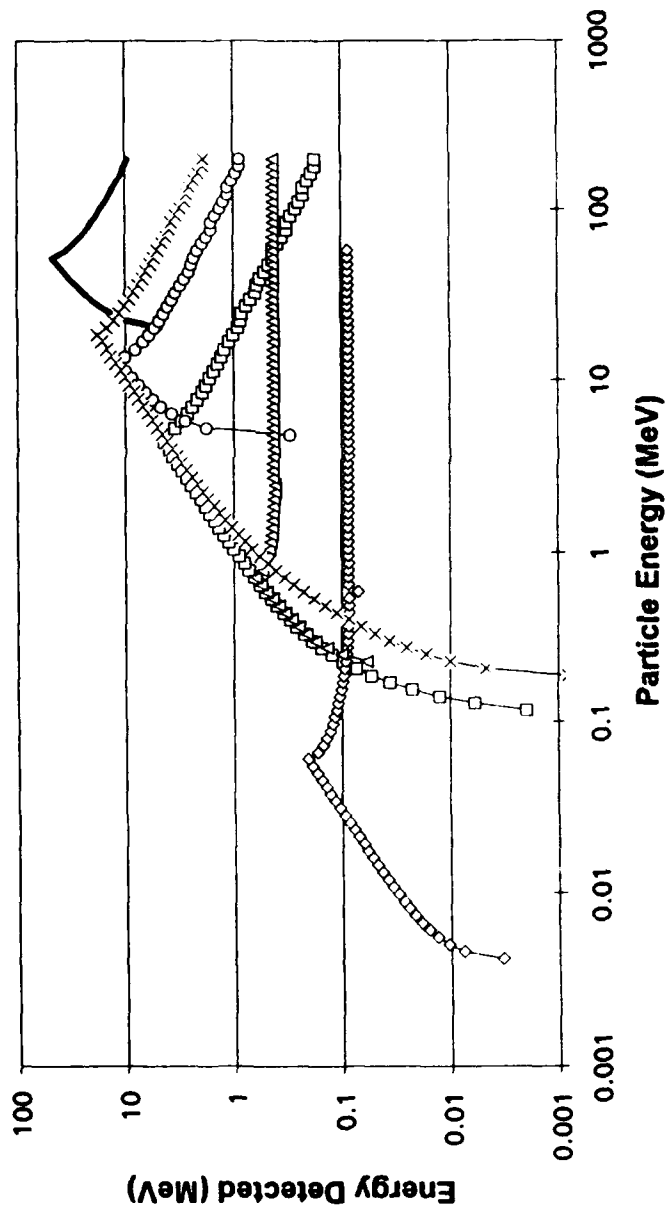
Run 2, 300, 150, 1000

Absorber: 700 ug/cm² Al
Front Detector: 34.5 ug/cm² Si(Dead Layer)/
34.5 mg/cm² Si(D1)/46 ug/cm² Si(Dead Layer)



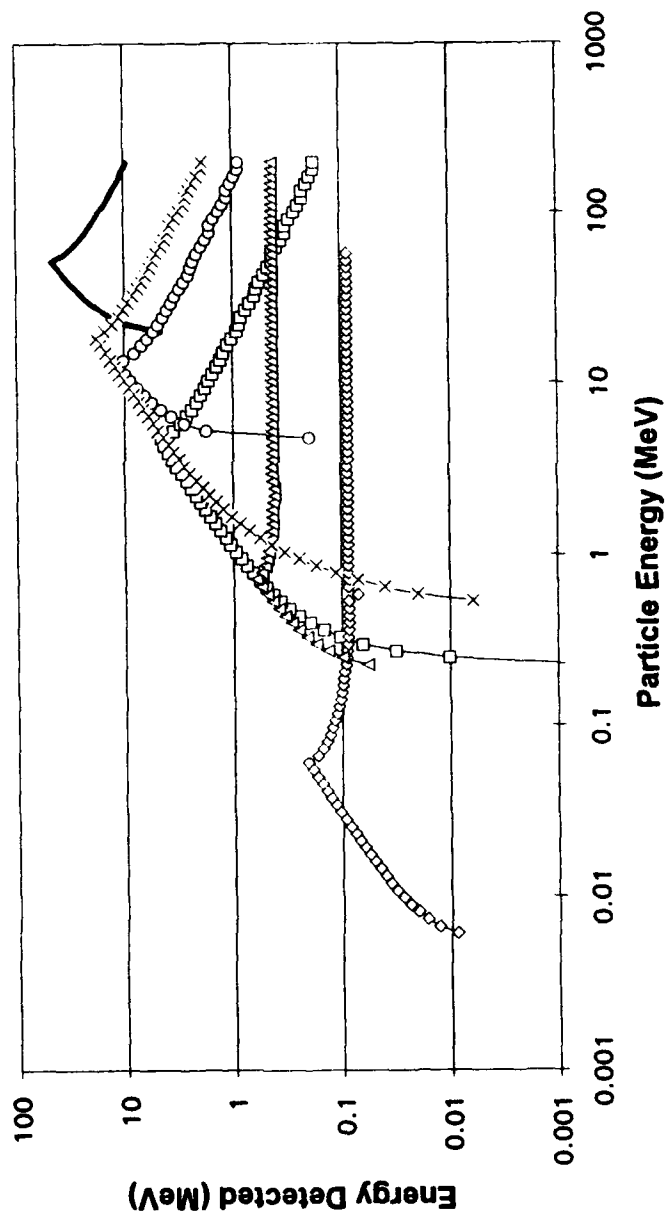
Run 2, 700, 150, 1000

Absorber: 300 ug/cm² Al
Front Detector: 34.5 ug/cm² Si(Dead Layer)/
46 mg/cm² Si(D1)/46 ug/cm² Si(Dead Layer)



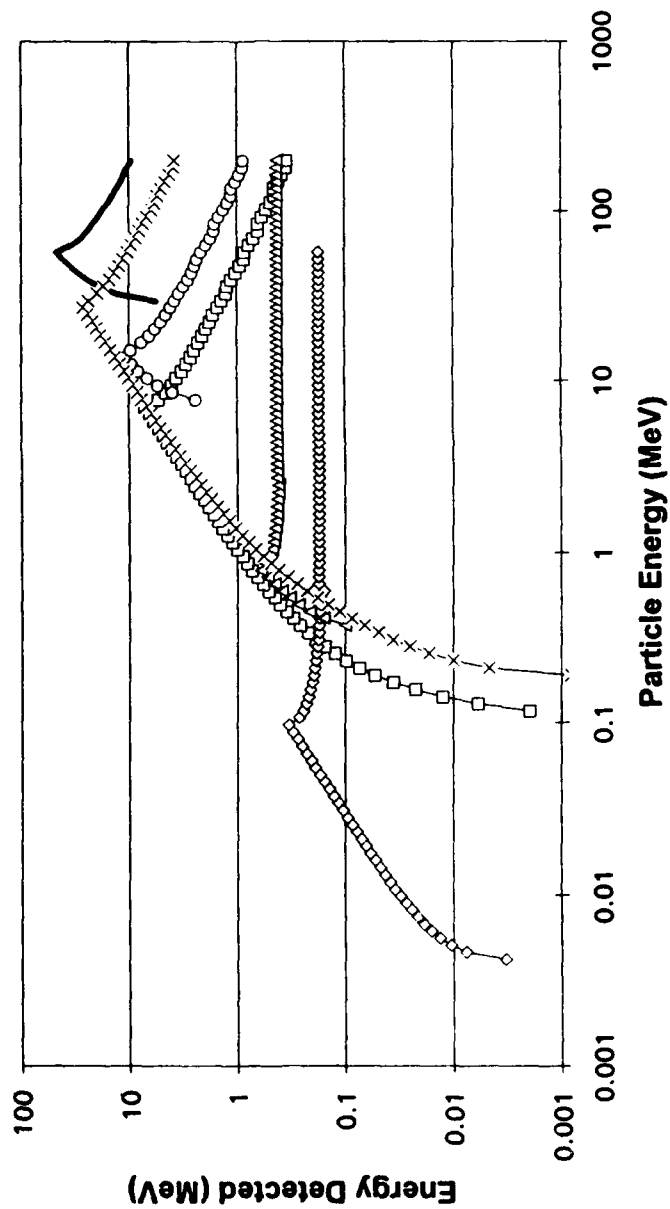
Run 3, 300, 200, 1000

Absorber: 600 ug/cm² Al
Front Detector: 34.5 ug/cm² Si(Dead Layer)/
46 mg/cm² Si(D1)/46 ug/cm² Si(Dead Layer)



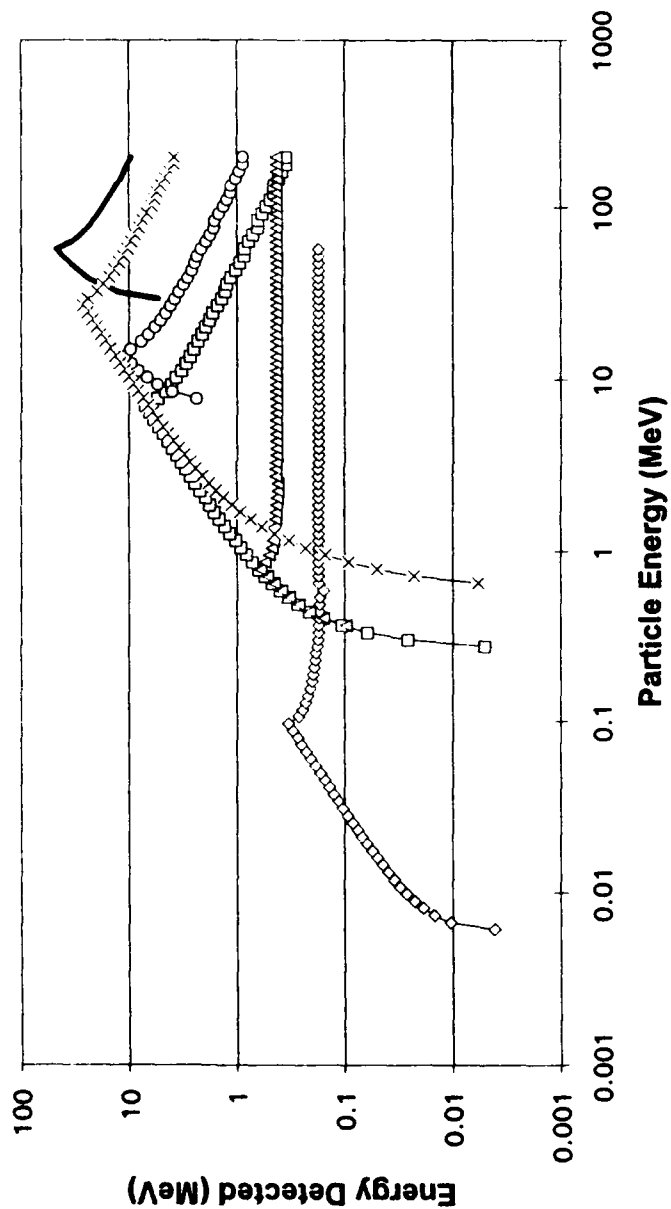
Run 3, 600, 200, 1000

Absorber: 300 ug/cm² Al
Front Detector: 34.5 ug/cm² Si(Dead Layer)/
92 mg/cm² Si(D1)/46 ug/cm² Si(Dead Layer)



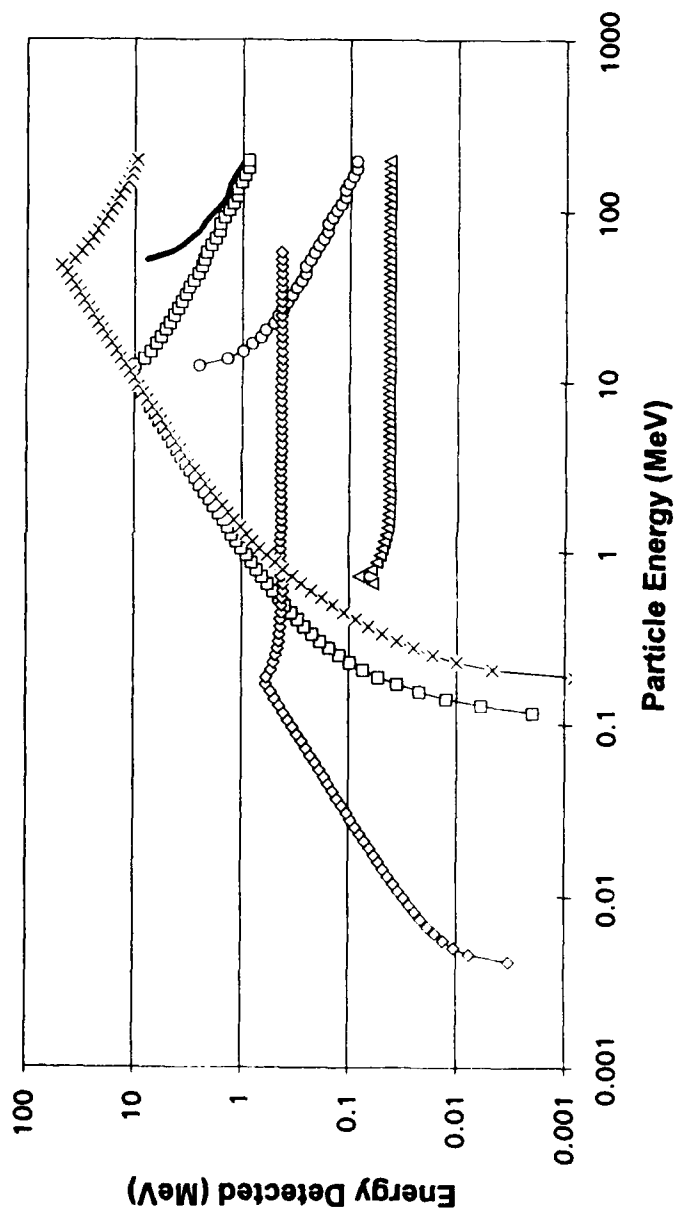
Run 4, 300, 400, 1000

Absorber: 700 ug/cm² Al
 Front Detector: 34.5 ug/cm² Si(Dead Layer)/
 92 mg/cm² Si(D1)/46 ug/cm² Si(Dead Layer)



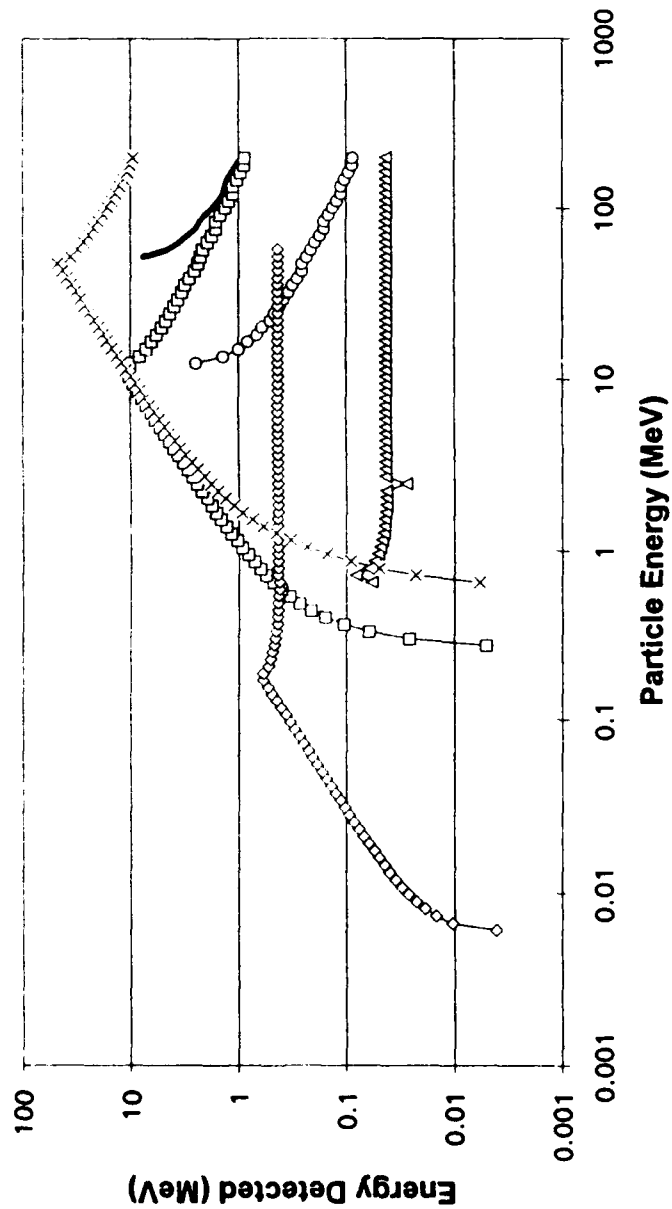
Run 4, 700, 400, 1000

Absorber: 300 ug/cm² Al
Front Detector: 34.5 ug/cm² Si(Dead Layer)/
230 mg/cm² Si(D1)/46 ug/cm² Si(Dead Layer)



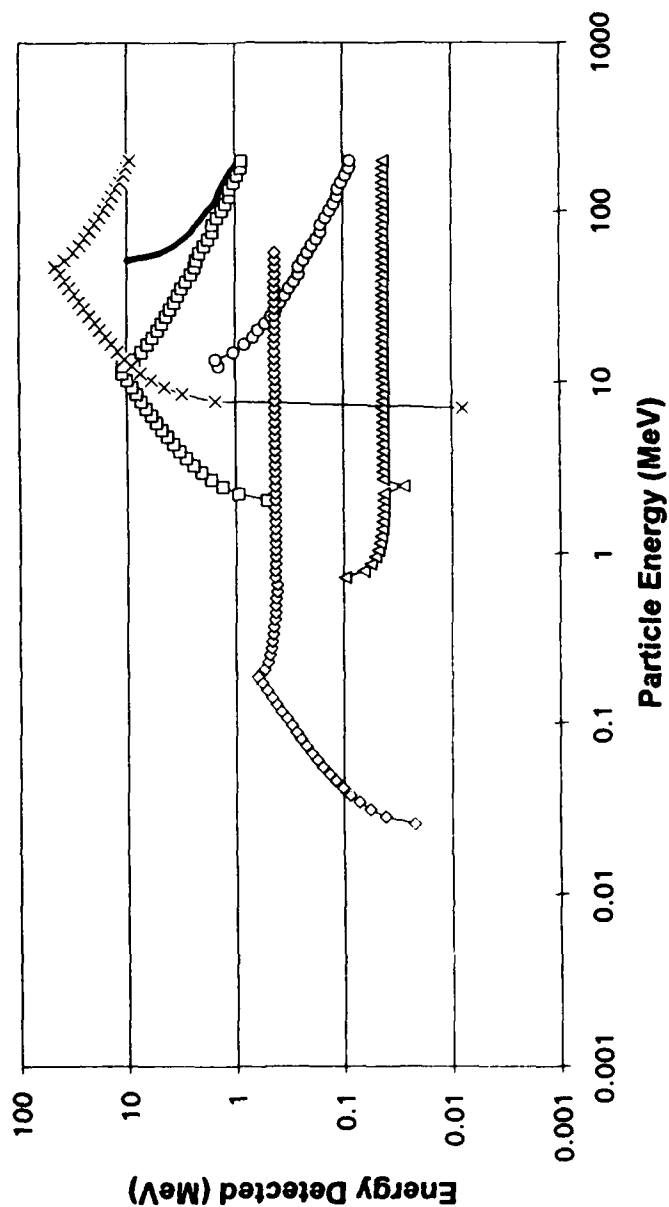
Run 5, 300, 1000, 100

Absorber: 700 ug/cm² Al
Front Detector: 34.5 ug/cm² Si(Dead Layer)/
230 mg/cm² Si(D1)/46 ug/cm² Si(Dead Layer)



Run 5, 700, 1000, 100

Absorber: 1000 ug/cm² Al
 Front Detector: 34.5 ug/cm² Si(Dead Layer)/
 230 mg/cm² Si(D1)/46 ug/cm² Si(Dead Layer)



Run 5, 10000, 1000, 100